January 2012

Galnt11 Is A Novel Galnac-Transferase That Glycosylates Notch1 Receptor To Specify Between Motor And Sensory Ciliary Fates In The Vertebrate Left-Right Organizer

Marko Boskovski
Yale School of Medicine, marko.boskovski@yale.edu

Galnt11 is a Novel GalNAc-transferase that Glycosylates Notch1 Receptor to Specify Between Motor and Sensory Ciliary Fates in the Vertebrate Left-Right Organizer

A Thesis Submitted to the

Yale University School of Medicine

In Partial Fulfillment of the Requirements for the

Degree of Doctor of Medicine

by

Marko T. Boskovski

2012

ABSTRACT

GALNT11 IS A NOVEL GALNAC-TRANSFERASE THAT GLYCOSYLATES NOTCH1 RECEPTOR TO SPECIFY BETWEEN MOTOR AND SENSORY CILIARY FATES IN THE VERTEBRATE LEFT-RIGHT ORGANIZER.

Marko T. Boskovski, Mustafa Khokha and Martina Brueckner. Section of Cardiology, Department of Pediatrics, Yale University, School of Medicine, New Haven, CT.

Heterotaxy is a disease of abnormal left-right (LR) body patterning associated with congenital heart disease that has very poor outcomes. Despite advances in surgical management, the two most severe forms of heterotaxy, right and left atrial isomerism, have a 29% and 64% 5-year survival rate, respectively. Through copy number variant analysis of heterotaxy patients, GALNT11 was recently identified as a novel gene important in human LR development. However, the mechanism by which *Galnt11* causes heterotaxy has not been elucidated. In order to discover the mechanism of GALNT11 in patterning the LR axis, I performed loss of function and gain of function studies in *Xenopus tropicalis* and expression analysis in *Mus musculus*. In Xenopus, knockdown of *galnt11* = induced heart looping defects that were successfully rescued with human GALNT11 mRNA indicating that the phenotype was specific to Galnt11. Via immunohistochemistry, Galnt11 protein strongly localizes to the crown cells surrounding the LRO. Manipulations of *Galnt11* altered the density of ciliated epidermal cells, but based on gliding assays and ultrastructural analysis did not alter the cilia. *Galnt11* and *Notch* effects on epidermal ciliated epidermal cell density, heart looping, as well as *PitX2* and *Coco* expression were very similar, and *Galnt11* morphants were rescued with *Notch ICD* and *Su(H)-Ank*, but not *Delta* suggesting that

galnt11 acts in the notch pathway downstream of the ligand. GALNT11 RNA no longer had any effect on heart looping or *PitX2* expression following a conservative point mutation of its catalytic glycosylation domain. *Galnt11* morphants had significantly narrower LROs, and much stronger expression of motile ciliary markers *FoxJ1* and *RFX2*, while GALNT11 RNA injected embryos had almost no detectable *FoxJ1* and *RFX2*. Taken together, these results indicate that Galnt11 is a GalNAc-transferase that is necessary for proper left-right axis establishment and heart looping. Its function is to specify between motile and sensory cell fates at the Left-Right Organizer by glycosylating Notch receptor and modifying Notch signaling.

Research and Thesis Faculty Mentors:

Martina Brueckner, M.D., Associate Professor of Pediatrics (Cardiology) and of Genetics

Mustafa Khokha, M.D., Associate Professor of Pediatrics (Critical Care) and of Genetics

ACKNOWLEDGEMENTS

Isaac Newton is said to have written, “If I have seen further it is by standing on the shoulders of giants.” It seems to me that every person’s accomplishments are achieved by standing on the shoulders of personal giants, for it is impossible to traverse this world in isolation. The following are the giants in my life without whom my research and this thesis would not have been possible.

During my first year in medical school, I was incredibly lucky to meet two masters of surgery, Dr. Arnar Geirsson and Dr. Richard Kim. Over the years they have become not only my mentors, but also dear friends. They have fueled my passion for surgery, pushed me to make the most out of my talents, and shown me first-hand what kind of a surgeon I should strive to become.

Dr. Martina Brueckner and Dr. Mustafa Khokha are the two best research mentors and friends one could ever ask for. They are extraordinary physician-scientists who have helped me experience the joy of scientific pursuit in a way that I could have never imagined. I would especially like to thank them for pointing out to me that perhaps my in situ hybridizations would work better if I mix the RNA probe with Hyb buffer as opposed to water.

The members of the Brueckner and Khokha Labs have been my family away from home. They have made my research time not only productive, but also incredibly enjoyable. I am especially indebted to Ms. Svetlana Makova for helping me transition from my previous research in biomedical physics to the world of developmental biology and genetics, as well as Dr. Khalid Fakhro who identified a copy number variant of galnt11 in a human heterotaxy

patient and opened the door to the many possibilities of how galnt11 may affect cell signaling.

Dr. John Forrest, Donna Carranzo and Mae Geter from the Office of Student Research deserve special recognition. They have enthusiastically supported the scientific pursuits of all Yale medical students, and are a big part of the reason why the Yale Medical School is a truly special place to learn medicine.

Last, but not the least, my family and friends, have been ardent supporters of my talents, goals and dreams.

My research and this thesis was made possible by Grant Number TL 1 RR024137 from the National Center for Research Resources (NCRR), a component of the National Institutes of Health (NIH) and NIH Roadmap for Medical Research. Its contents are solely the responsibility of the authors and do not necessarily represent office views of NCRR or NIH.

Marko T. Boskovski

Yale University School of Medicine

New Haven, Connecticut, USA

TABLE OF CONTENTS

I. INTRODUCTION

I.1. *Heterotaxy Syndrome*

The heart is the most visibly asymmetric organ in the human body. It is positioned in the left chest, and is tilted such that the apex points in a left antero-inferior direction, thereby placing the right ventricle most anterior and the left atrium most posterior but anterior of the trachea. Following the blood flow, the heart has asymmetric venous drainage into the atria. The superior and inferior vena cava drain into the right atrium, while four pulmonary veins drain into the left atrium. The blood then goes through the asymmetrically coiled semilunar valves – the bicuspid mitral valve on the left and the tricuspid valve on the right to enter the ventricles, which are not only asymmetrically oriented, but also anatomically and functionally distinct. The ventricles then pump blood through the aortic and pulmonary valves into the asymmetrically coiled great vessels. It is obvious then, that precise developmental asymmetry across the left-right (LR) axis is essential for proper heart function.

Failure to properly develop LR asymmetry leads to a group of disorders that are collectively referred to as heterotaxy syndrome. In heterotaxy, organs or asymmetric structures within organs fail to properly align relative to each other. Given the highly asymmetric structure of the heart itself, and the structures surrounding the heart, failure of these processes results in a plethora of congenital heart disease.

Positioning along the LR axis can be divided into three broad categories (Fig. 1). Situs solitus refers to the proper alignment of organs across the LR axis. Situs inversus, with an incidence of 1 in 8500 in the general population, refers to a mirror image arrangement of organs across the LR axis when compared to situs solitus, and is not usually associated with

intra-cardiac defects. Heterotaxy covers the spectrum of LR axis malformations that fall in between situs solitus and situs inversus. It has an incidence of 1 in 10,000 in the general population, and has a very high association with intra-cardiac defects.[1]

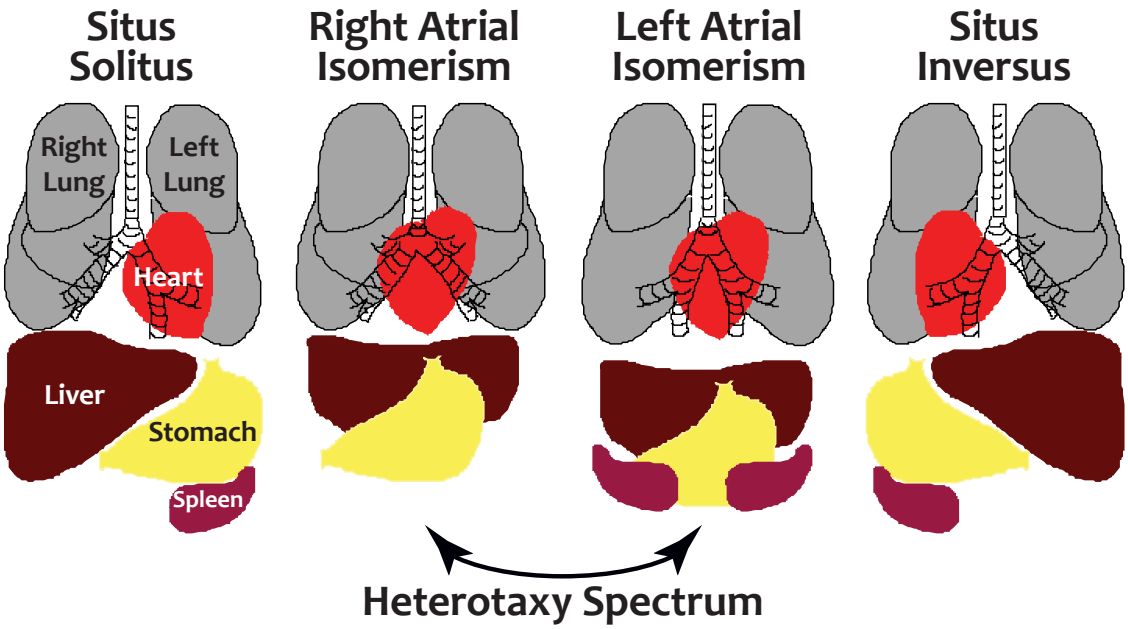

Figure 1. A schematic representation of the spectrum of heterotaxy disorders. Situs solitus on the left represents normal organ arrangement across the LR axis, while situs inversus on the right is its mirror image. Any organ or intraorgan arrangement in between situs solitus and situs inversus is considered heterotaxy, represented by right and left atrial isomerism in the middle two panels. Reproduced with permission from Martina Brueckner.

Heterotaxy itself represents a range of disorders. In minor cases there is partial development of asymmetry where there is discordance between organs (e.g. isolated dextrocardia with abdominal situs solitus) or discordance within one organ (e.g. isolated levo transposition of the great vessels with a levo-ventricular loop and normal atrial and abdominal situs). The most severe cases result from complete failure to develop asymmetry across the LR axis in the whole body, thus leading to Ivemark syndrome, also referred to as right and left atrial isomerisms. In essence, in right atrial isomerism the body has two "right" sides (with bilateral right atria), while in left atrial isomerism the body has two "left" sides (with bilateral

left atria). The intracardiac anatomy in isomerism is highly complex, with intracardiac defects found in 83% of left atrial isomerism and 100% of right atrial isomerism diagnosed prenatally.[2] The most prevalent defect across both left and right atrial isomerism is an atrioventricular septal defect, affecting from 60% to 100% of patients. Complex abnormalities of systemic and pulmonary venous drainage, along with malposition of the great vessels and subpulmonary or aortic obstruction, coexist in the majority of cases. The long-term outcome for patients with isomerism has remained poor despite improvements in the medical and surgical management of other congenital heart disease: the 5-year survival for patients with left atrial isomerism and right atrial isomerism is reported to be only 64% and 29%, respectively.[3]

Given the prevalence and severity of disease in heterotaxy, an understanding of LR patterning in vertebrate model organisms is essential. Such understanding has the potential to not only help us delineate the pathogenesis of different heterotaxy cases, but with recent advances in genetic sequencing, also inform us about the prognosis and treatment of these patients.

I.2. *Overview of vertebrate left-right asymmetry development*

In vertebrates, the LR axis develops through a highly organized and regulated series of events. In simple terms, this process can be divided into three broad stages. The first involves the LRO, a transient, ciliated organ present early in development, which creates asymmetric cilia driven flow. This event represents the initial symmetry breaking point across the LR axis. The second stage involves asymmetric gene expression, which is induced by the asymmetric flow. This differential gene expression is then propagated throughout

embryo development to instruct the third and final event in embryo development: asymmetric organogenesis.

As is the case with all of biology, this simple scaffold is overlaid with a myriad of regulatory mechanisms, including Notch, Nodal, Hedgehog, FGF, Wnt and BMP.[4-7] In the past decade, Notch signaling has emerged as a central regulatory component at several points during the LR developmental cascade.

This introduction will first cover in detail the three broad stages of LR development, followed by a discussion on Notch signaling in general and more specifically as it applies to LR development. The focus will then shift to the genetics of heterotaxy and how recent findings from heterotaxy patients have revolutionized the field of LR development. The introduction will conclude with a discussion on Galnt11, a novel glycosylation factor that was identified through a copy number variant analysis of heterotaxy patients which I have demonstrated to affect LR patterning via the Notch pathway.

I.3. *The LRO is a conserved ciliated signaling center that breaks LR asymmetry*

Despite the significantly different anatomy of various vertebrate species, central to the first stage of LR development is a conserved, homologous vertebrate structure called the Hensen's node in chick,[8] node in mouse,[9] posterior notochord (PNC) in rabbit,[10,11] Kuppfer's vesicle (KV) in fish,[10] and gastrocoel roof plate (GRP) in frog,[12] which we will collectively refer to as the left-right organizer (LRO) (Fig.2). The LRO forms towards the end of gastrulation and is composed of 50-250 monociliated cells. The synchronized rotation of the cilia on these cells creates a leftward laminar fluid flow of the extracellular fluid above the LRO (Fig. 3).[13] Using high-speed video microscopy, in the mouse the LRO cilia have been

observed to rotate at a speed of 600 rpm to drive a flow of ~15-20 µm/second.[13] Similarly, the LRO flow has been observed in frog by tracking fluorescent beads.[12] The end result of this leftward flow is the induction of the second stage of LR development, asymmetric gene expression.

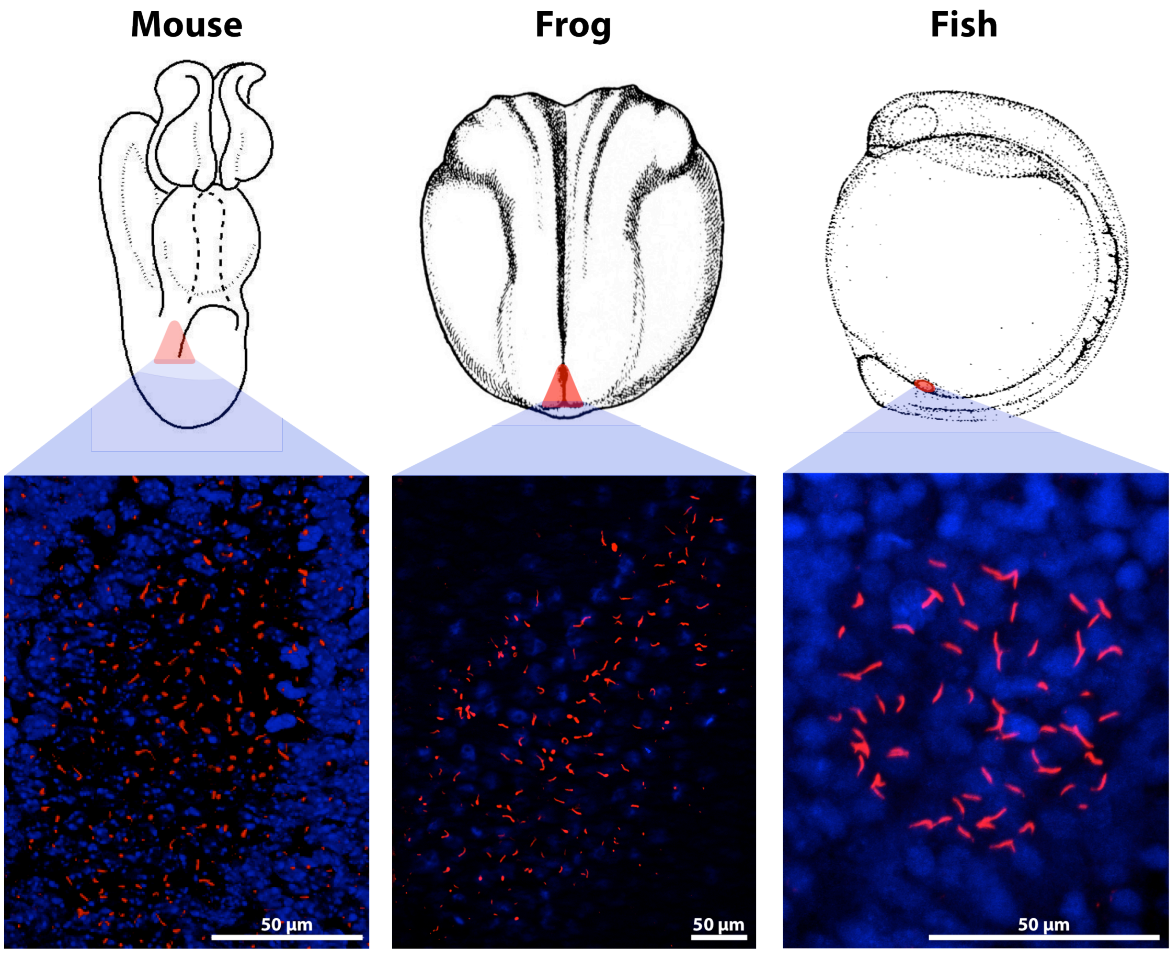

Figure 2. Comparison of the LRO in different vertebrate species. **A-C** Diagrams of developing mouse, frog and fish embryos. The location of the LRO is outlined in red. **D-F** Immunofluorescence pictures of the corresponding LRO. Monocilia are labeled with acetylated tubulin (red) and cell nuclei are labeled with Hoechst (blue).

There are several lines of evidence supporting that the LRO is a homologous structure that is conserved throughout vertebrate species. A ciliated LRO organizer has been identified in every major vertebrate model system (Fig. 2), although it has been difficult to definitively

identify the ciliated LRO in chick.[14] In each case, the cilia have been documented to be motile, and consequently, to produce leftward flow. Furthermore, it is always derived from the superficial mesoderm and has flanking expression of homologs of the gene *Nodal* (discussed below). Finally, mechanical destruction of LRO precursor cells in frog,[15] or the LRO itself in zebrafish[10] yields laterality defects (i.e. situs inversus and heterotaxy) in the face of normal AP and DV development, indicating that the LRO is not only a conserved structure, but also one that is required for normal LR development. The ciliated LRO has not actually been visualized in the human embryo for obvious ethical reasons; however, a combination of the remarkable conservation of a cilia-driven flow mechanism for initiating LR asymmetry in vertebrates, and the association between human ciliopathies (see below) and situs abnormalities, makes it highly likely that there is an LRO in the early human embryo also.

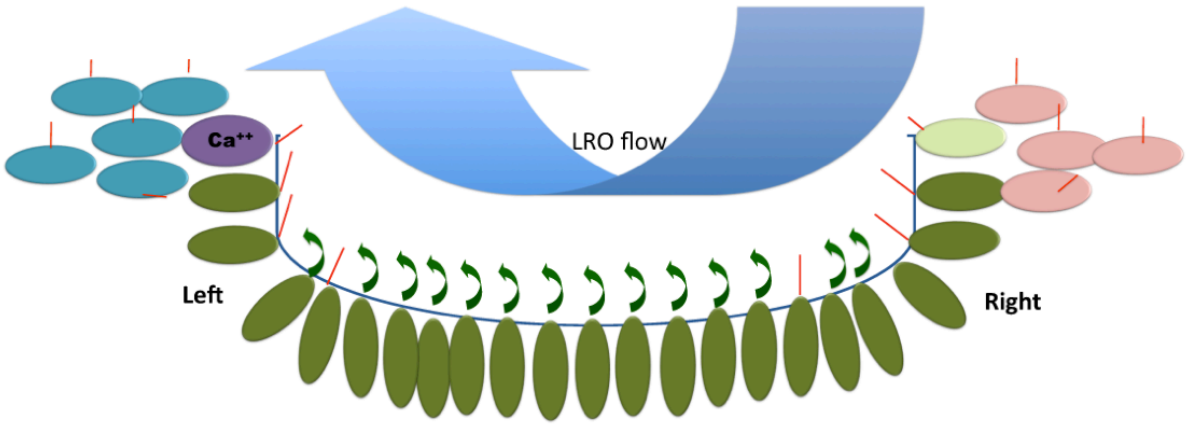

Figure 3. Schematic of the mouse LRO. Motile cilia on pit cells (shown with green arrows on dark gray cells) generate leftward flow of extracellular fluid (shown as blue arrow). Sensory cilia on crown cells (shown as red arrows on light gray cells) transduce flow information into asymmetric signals, including increased intracellular calcium in the cells at the left. This leads to subsequent asymmetric gene expression.

I.4. ***LRO cilia are chiral organelles that induce LR asymmetry from positional cues derived from the AP and DV axes***

The LR axis is unique in that it is defined with respect to the anteroposterior (AP) and dorsoventral (DV) axes. Therefore, the embryo must have mechanisms to both create asymmetry and to consistently align the asymmetry with the existing AP and DV axes. This predicts that failure to create asymmetry results in retained bilateral symmetry, manifesting as left or right atrial isomerism. In contrast, inability to align the asymmetry manifests as random asymmetry, such as the 50% incidence of situs inversus totalis observed in patients with primary ciliary dyskinesia. Wilhelmi originally proposed that the organism has an underlying mechanism that generates random asymmetry.[16] Brown and Wolpert hypothesized that this asymmetry is biased in a consistent direction by the presence of a handed asymmetric molecule or macromolecular structure that can align with the AP and DV axes, which they represented by the letter "F".[17]

Extensive work in model systems including zebrafish, *Xenopus* and mouse indicates that the initial handed reference structure is the cilium, a highly chiral organelle that is found on almost all cells. Specifically, it is the cilia positioned on the ventral surface of the LRO that orient the LR axis relative to the established AP and DV axes. This is established through the rotational angle of the cilia, which in separate studies have been found to be tilted 40 ± 10° and 15–35° posteriorly in mouse.[18,19] Hemodynamic principles dictate that if cilia are uniformly tilted in a specific direction, then it is possible to create unidirectional flow with rotational ciliary motion through a no-slip boundary effect.[20] When cilia move closer to the surface, the movement of the fluid they drive will be retarded by the viscous forces of the stationary fluid that is in immediate contact with the surface. Conversely, when

the same cilia move in the opposite direction away from the surface, they can freely drive the fluid with no opposing forces due to static surfaces.[21-24] The end result is unidirectional motion in the direction of the halfstroke when the cilium is oriented away from the cell surface. In the case of the LRO, the cilia are tilted posteriorly and they rotate in a clockwise direction. According to the principles described above, almost no fluid flow is generated on the rightward half-stroke when the cilia are close to the surface, and robust fluid flow is generated on the leftward half-stroke when the cilia are away from the surface, thereby creating the overall leftward fluid flow that is observed.

It becomes apparent then, that proper development of both the AP and DV axes are required for correct LR patterning. The DV axis instructs the protrusion of cilia on the ventral side of the LRO,[9] while the AP axis is necessary for proper posterior tilt. The answer to how a posterior tilt is achieved lies in the spherical shape of the LRO cells containing motile cilia. A careful examination of these cells in both mouse and frog reveals that the basal bodies and the cilia are located posteriorly, thereby forcing a posterior tilt of the cilium as it protrudes outside.[18,19]

I.5. *Structure and Function of Cilia*

Essential for normal LRO function and subsequent normal LR development is the proper function of the LRO monocilia. Cilia, in general, are large, complex organelles that, depending on the tissue they are found in, protrude up to 20μm beyond the cytoplasm.[25] They are composed of the ciliary axoneme surrounded by the ciliary membrane, which is contiguous with the plasma membrane. The axoneme comprises the microtubule skeleton consisting of 9 microtubule (MT) doublets with attached intraflagellar transport (IFT)

proteins. Since there is no protein synthesis in cilia, IFT proteins are required to selectively transport the structural and functional components of cilia from the cytoplasm into the axoneme, and to return products of ciliary signaling to the cytoplasm (Fig. 4).

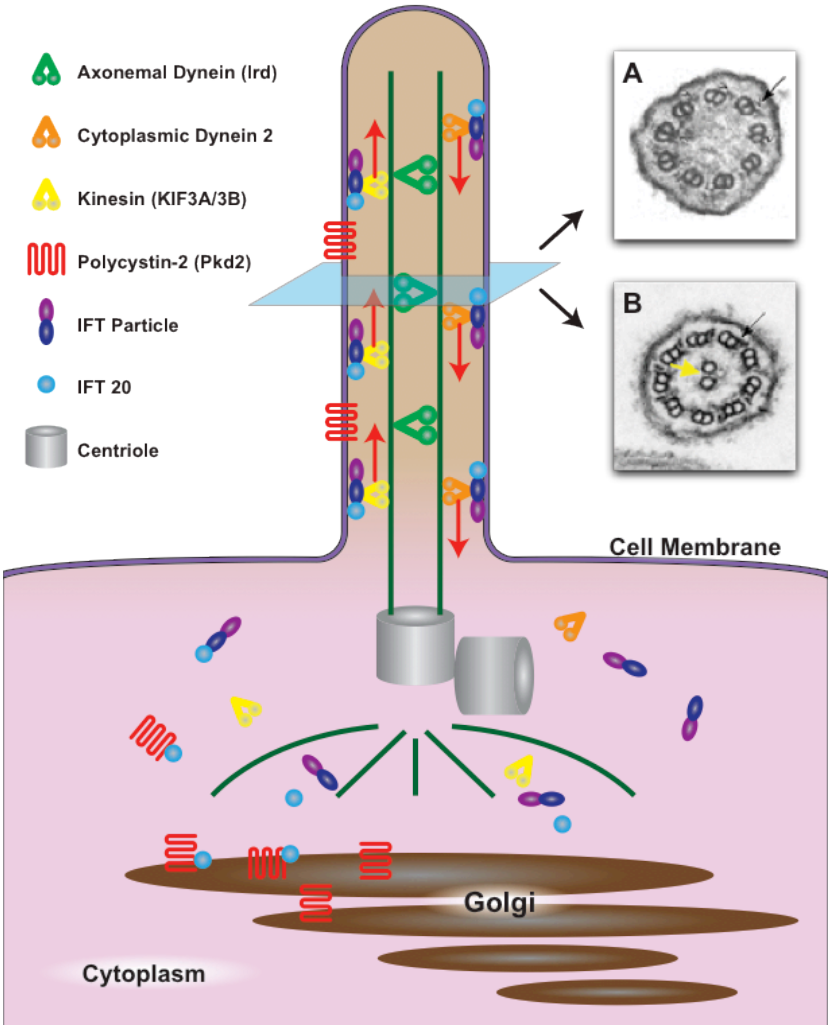

Figure 4. Schematic representation of a cilium. The microtubule based structure is assembled at the basal body (epithelial cilia) or the mother centriole (monocilia). Proteins necessary for proper ciliary function go from the Golgi to the base of the cilium via IFT proteins where they are transported up the cilium in anterograde fashion by kinesin motor proteins, and down the cilium in retrograde fashion by the dynein motor proteins. Inset **A** Electron micrograph (EM) of a monocilium lacking a central microtubule pair **B** EM of a motile epithelial cilium with a central microtubule pair.

Cilia can be subdivided into epithelial cilia and primary cilia. Epithelial cilia, such as those found on the apical surface of epithelial cells of the trachea, choroid plexus and oviduct, contain motor proteins, as well as a central pair of MTs linked by radial spokes to the outer 9 doublets. The motor proteins – a combination of outer and inner arm dynein motors – along with their associated dynein regulatory proteins, hydrolyze ATP to generate ciliary movement. Typically there are many cilia per epithelial cell that arise from basal bodies beneath the cell membrane, which themselves originate from the template of the mother centriole. The concerted action of large numbers of closely spaced motile cilia transports surrounding fluid, such as tracheal secretions or cerebrospinal fluid.

In contrast to the highly specialized epithelial cilia, almost all cells (with the exception of a few myeloid and lymphoid lines) can carry primary cilia (also known as monocilia). As the name suggests, there is only one monocilium per cell, which arises directly from the mother centriole. Like the cilia found in ciliated epithelia, the axoneme of primary cilia is constructed on a scaffold consisting of 9 MT doublets. Unlike the stereotypical arrangement of microtubules, motors and structural proteins found in epithelial cilia, the contents of monocilia are extremely varied. As such, monocilia can serve different functions depending on the proteins they are loaded with. For example, by displaying specialized receptors, these cilia are adapted to function as light photoreceptors in the retina, or as olfactory receptors in the nose. Primary cilia are also signaling centers at the interface between the cell and the extracellular environment. For example, they are essential for hedgehog signaling, and absent or defective cilia in mouse embryos result in a spectrum of defects including neural tube defects, polydactyly and cardiac defects.[26,27]

In the LRO, there are two different types of primary cilia: motile and sensory (Fig. 3). The motile primary cilia, which populate the center of the LRO, are equipped with dynein motor proteins, enabling them to create a leftward fluid flow and break LR symmetry. The non-motile monocilia are more abundant at the lateral edge of the LRO in mouse, and lack dynein motor proteins, but contain polycystin-2, the product of the gene mutated in type 2 dominant polycystic kidney disease.[28] It is a cation channel that is required to sense the flow generated by the motile monocilia.[29] In the presence of leftward LRO flow, polycystin-2 induces an increase in calcium concentration on the left LRO border, and therefore translates the LRO flow into an asymmetric calcium gradient.[28]

There is significant evidence to support the model outlined above that 1) flow generated by LRO monocilia is required for proper LR patterning and 2) that sensory cilia detect this leftward flow. First, regarding the requirement for motile cilia at the LRO, altered function (i.e. mutations, knockdown or knockout) of any of a number of ciliary genes including components of the dynein motor complex or genes necessary for ciliary biogenesis such as the IFTs results in LR patterning defects.[13,30-33] Initial evidence for a role of cilia in development of LR asymmetry came from study of patients with Primary Ciliary Dyskinesia (Kartagener syndrome), which manifests as respiratory disease, male infertility and a 50% incidence of situs inversus.[34] Respiratory compromise and male infertility in PCD are due to defective dynein function in the tracheal cilia and sperm axoneme, while randomization of SS and SI is secondary to improper LRO motile cilia function. Similarly, mice with a point mutation in the left-right dynein (*lrd*) gene, which renders cilia immotile, also have randomization of SS and SI.[30] LRO flow in these mice is absent, but artificial application of leftward flow across the LRO can re-establish SS, while application of flow to the right can

induce SI.[35] This indicates that LRO flow itself is the event that breaks LR symmetry. Second, regarding the requirement for sensory cilia at the LRO, mice that lack LRO flow due to immotile cilia have been shown to lack increased calcium levels on the left border of the LRO. This is also the case in mice with normal LRO flow that lack the *polycystin-2* gene, indicating that there are no asymmetric calcium levels in the absence of leftward LRO flow, and that detection of LRO flow requires the presence of the polycystin-2 receptors in the surrounding sensory cilia.[28]

I.6. *Asymmetric gene expression downstream from the LRO*

The result of asymmetric LRO flow is a downstream cascade of asymmetric gene expression that propagates the asymmetric signal and ultimately results in asymmetric organogenesis. This cascade is outlined by asymmetric expression of *Coco*, *Nodal*, *Lefty-1*, *Lefty-2* and *PitX2*, all of which are observed prior to visible asymmetry of heart looping (Fig. 5).

Nodal is a left-side determinant that is initially expressed symmetrically around the LRO.[36-39] It subsequently becomes asymmetrically expressed at both the LRO and the left lateral plate mesoderm (LPM), a structure lateral to the LRO that later contributes to the mesenchyme of various visceral organs. Cells in the left LPM that receive Nodal signaling contribute to various visceral organs, such as the lung and heart, that develop left-side specific morphologies. On the other hand, in the absence of *Nodal* expression, both the left and right LPM specify right-sided organogenesis by default. In normal development peri-LRO *Nodal* expression induces its own expression at the left LPM through a positive feedback loop, thereby changing the default state of the left LPM from right to left-sided

organ development. With that in mind, complete absence of *Nodal* expression at both LPMs leads to the development of right atrial isomerism, while bilateral *Nodal* expression results in left atrial isomerism.

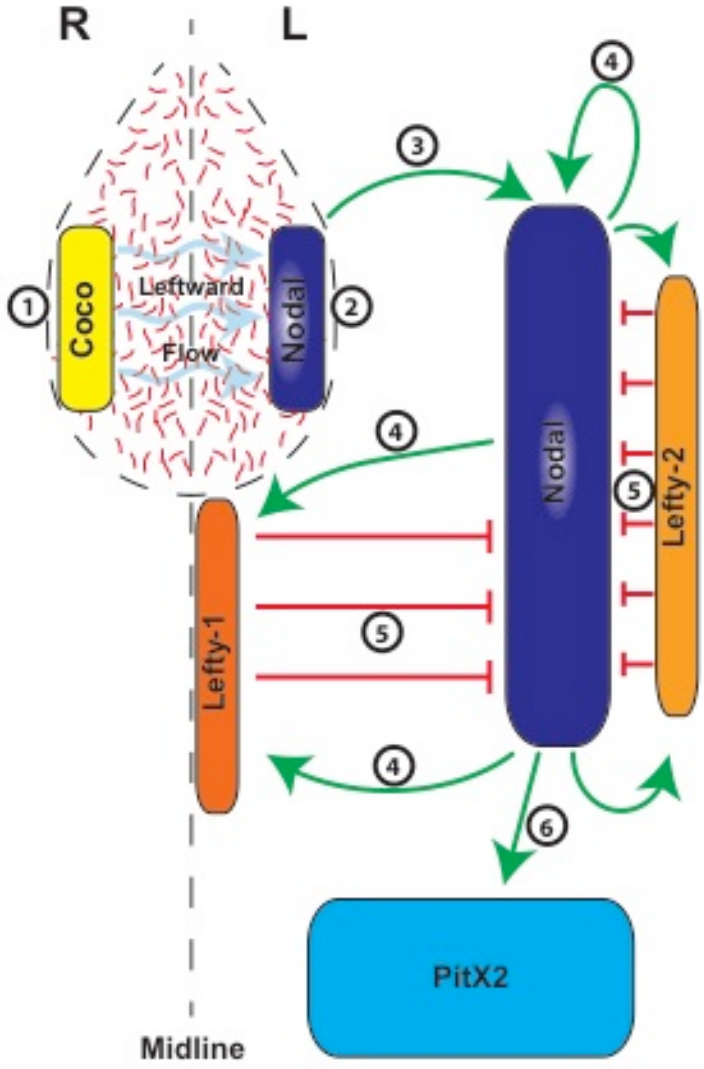

Figure 5. Schematic representation of the asymmetric gene cascade. **1**. At the LRO, leftward flow inhibits *Coco* (shown in yellow) expression on the left but not on the right. **2.** *Coco* inhibits *Nodal* (shown in dark blue) expression on the right but not the left. **3.** Left-sided *Nodal* expression at the LRO induces *Nodal* expression at the left LPM. **4.** *Nodal* induces its own expression, as well as the expression of *Lefty-1* and *Lefty-2* (shown in orange. **5.** *Lefty-1* and *Lefty-2* contain the expression of *Nodal* to the LPM. **6.** Left-sided *Nodal* expression induces left-sided *PitX2* expression (shown in light blue).

While leftward LRO flow is required for left LPM *Nodal* expression, *Nodal* itself does not directly respond to flow.[40] The transition from symmetric to asymmetric *Nodal* expression is mediated by *Coco* – a secreted antagonist of *Nodal.*[41-43] Before LRO flow is established, *Coco* and *Nodal* have overlapping, symmetric, peri-LRO patterns of expression. Unlike *Nodal*, *Coco* is directly inhibited by LRO flow. As a result, *Coco* is suppressed on the left, but still maintained on the right. Consequently, Coco releases its negative inhibition of the co-expressed *Nodal* protein, such that *Nodal* becomes asymmetrically expressed on the left, but not the right.[40]

Lefty-1 and *Lefty-2* are also *Nodal* inhibitors that are responsible for keeping the *Nodal* positive feedback loop in control, and its expression localized to the LPM.[44-46] They are induced by *Nodal* and are expressed at the midline (*Lefty-1*) and the left LPM (*Lefty-2*). In the absence of either gene, *Nodal* expression begins normally in the left LPM, but subsequently leaks to the other side.

The feedback inhibition of *Lefty-1* and *Lefty-2* not only limits the area of *Nodal* expression, but also the time. In the mouse, *Nodal* expression is present for only 6 hours. Once *Nodal* expression at the LPM ceases, it passes on the left-side determinant baton to another asymmetrically expressed gene *PitX2*.[47-49] *PitX2* is induced by *Nodal* at the LPM. However, it persists much longer, and once *Nodal* disappears its expression is maintained by *Nkx2*. As a left side determinant, similar to *Nodal*, complete absence of *PitX2* yields right atrial isomerism, while bilateral presence results in left atrial isomerism.

In this introduction, we have reviewed the roles of ciliary and TGF-beta signaling on LR development. Another critical pathway for LR patterning is the Notch pathway and is particularly relevant for the work in this thesis.

I.7. ***Molecular basis of Notch signaling***

The notch signaling pathway was first identified almost 100 years ago in mutant flies with "notched" wings.[50] It represents a local communication system between neighboring cells that is evolutionarily conserved and pervasive throughout development. Often responsible for the development of cell fate boundaries, such as the boundary between the anterior and posterior drosophila wing, and patterned structures such as the ciliated epithelium of *Xenopus*, Notch signaling is involved in a diverse range of biological processes such as cell-fate specification, self-renewal, differentiation, proliferation and apoptosis.

At the most basic level, the Notch signaling pathway consists of three core components which were originally discovered in mutant animals that phenocopied Notch mutants: 1) a Delta-type or Jagged/Serrate family ligand, 2) a Notch receptor, and 3) a CSL family transcription factor. Different species have a different number of each of these components. For example, there are four Notch receptors in human and mouse, three in Xenopus and one in drosophila. However, at least one ortholog of each of the three core components has been identified in all metazoan organisms studied to date.

The signaling process begins through the interaction of a delta-type or Jagged/Serrate ligand with a Notch receptor. In the majority of cases Notch ligands act as agonists, where they induce a complex series of proteolytic cleavages that release the Notch intracellular domain (NICD), which then translocates to the nucleus and binds to a CSL family transcription factor to affect target gene transcription. However, both types of ligands have also been described to act as antagonists of Notch signaling, although the mechanism of action is not as clearly understood as that for Notch activation.[51-57] It appears to be strictly

cell autonomous, such that cells expressing high levels of ligand can activate Notch signaling in neighboring cells, but prevent Notch activation in the cell they are expressed in.

Both Delta, Jagged/Serrate and Notch are single pass transmembrane proteins, with extracellular domains that contain arrays of multiple epidermal growth factor (EGF) - like repeats that mediate the interaction between the two proteins.[58] Next to the EGF repeats, Notch receptors also contain a negative regulatory region (NRR) and a heterodimerization (HD) domain, which serves to prevent Notch cleavage in the absence of ligand.[59] The full length Notch protein matures in the secretory pathway where it is cleaved by furin proteases at the S1 site located within the HD domain.[60,61] Subsequently, it is reassembled into a functional heterodimeric receptor at the cell surface where it is held together by non-covalent interactions.

The intricate process of Notch receptor activation and NICD release involves a series of four proteolytic cleavage events termed S1, S2, S3 and S4. Following interaction with a Notch ligand, the NECD-ligand complex gets endocytosed by the ligand-expressing cell, thereby applying a mechanical force that results in dissociation of the NECD/Notch transmembrane complex. The dissociation exposes the S2 site, which is located 12 amino acids proximal to the transmembrance domain of NTMIC,[62-64] thus enabling cleavage of the S2 site by ADAM10 or ADAM17 metalloproteases, which create a membrane tethered intermediate Notch extracellular truncation (NEXT).[65] Finally, a γ-secretase complex (composed of presenilin-1or -2, Aph1, Pen2, and Nicastrin) first cleaves the S3 site within the transmembrane domain, and then the S4 site, thereby releasing the NICD.[66,67]

Once released NICD translocates to the nucleus where it interacts with CSL, a family of sequence specific DNA binding proteins. In an unbound state, CSL proteins act as co-

repressors,[68] but once bound to NICD, they transform into co-activators.[69] This is achieved through distinct CSL co-activator and co-repressor complexes that are coordinated by NICD, such that in the absence of NICD CSL proteins associate with co-repressors, whereas in the presence of NICD they associate with co-activators. The use of co-repressor/co-activator complexes also allows for cell-type and time specific Notch signaling by requiring additional co-factors that are specific for different Notch target genes.

This type of Notch signaling control can lead to unexpected and counterintuitive results during experimental manipulation. A decrease in Notch signaling via knockdown or knockout of Notch components would be expected to lead to lower expression of Notch target genes, as has been observed in Notch mutants. However, CSL mutants can have a milder phenotype than Notch mutants, because of the cancelling effects of removing both the co-repressive and co-activating function of CSL proteins. In some cases, CSL mutants have a higher level of Notch target gene expression because of dual regulation by both CSL proteins, as well as other transcription factors that become upregulated when Notch signaling is compromised.[70] Similar results have been observed in Notch ligand mutants where the dominant action of the ligand is as an antagonist and not agonist.[51-57] Finally, overexpression of NICD leads to ectopic expression of Notch target genes only sometimes, because certain Notch target genes require additional co-factors (that may be lacking in ectopic tissues) for proper CSL co-activator complex function.[71,72]

I.8. ***Notch forms cell boundaries and patterned structures***

While Notch signaling is used for many different cell-fate decisions, most instances fall into one of three categories: lateral inhibition, decisions on cell lineage and inductive

signaling.[73-76] Lateral inhibition yields a "dotted" pattern of a particular cell fate among a surrounding group of cells of a different cell fate, as seen, for example, on the surface of the ciliated frog epidermis. A group of equipotent cells signal to each other via Notch signaling to inhibit each other from adopting a specific cell fate. In the case of the ciliated frog epidermis, a ciliated cell ends up expressing greater quantities of Notch ligand, which induces Notch signaling in neighboring cells that inhibits cilia formation. Additionally, it also leads to down-regulation of Notch ligand in the surrounding, non-ciliated cells, in order to prevent induction of Notch signaling in the ciliated cell.

Lineage decisions typically occur through asymmetric cell divisions. One daughter cell has activated Notch signaling, while the other does not. As a result the two cells adopt different cell fates. Finally, inductive signaling is often responsible for the creation of borders, such as the border between the anterior and posterior portions of the drosophila wing. One group of cells of a distinct lineage signals a bordering group of cells and "induces" a different cell fate, thereby creating a border.[77] The border is maintained through unidirectional Notch signaling and feedback loops, similar to the scenario described in lateral inhibition. One group of cells expresses a high level of Notch ligand and receives very little Notch signaling, while the neighboring group of cells has a high level of Notch signaling that induces a different cell fate, and inhibits expression of Notch ligand.

I.9. ***Regulation of Notch signaling via glycosylation***

While most extracellular proteins undergo *N*-linked glycosylation, the extracellular domain of Notch also undergoes a unique form of *O*-linked glycosylation that is essential for Notch signaling and its modulation. Two different types of *O*-glycosylation have been

observed on Notch, either with *O*-linked glucose or *O*-linked fucose. While the significance, if any, of *O*-linked glucose is still unclear, *O*-linked fucose can influence Notch signaling.[78-80]

O-glucoylation and *O*-fucosylation were first discovered on a different class of proteins that, like Notch, also carry repeating EGF domains – serum glycoproteins that are involved in regulating blood clotting and fibrinolysis.[81] This led to the observation that the extracellular domain of Notch also carries *O*-glucose and *O*-fucose, which can then extended by glycosyltransferases to form trisaccharide and tetrasaccharide chains, respectively.[82] The initial glycosylation of Notch by *O*-fucose is essential for Notch signaling, while the subsequent addition of the second, third and fourth sugars is not required, but can modulate the sensitivity of the Notch receptor to different ligands.

The enzyme O-FucT-1, encoded in mammals by the gene protein *O*-fucosyltransferase 1 (*POFUT1*), catalyzes the initial addition of *O*-fucose to an EGF domain.[83,84] There is a single *POFUT1* gene in mammals, *C. elegans,* and *Drosophila*.[84] O-FucT-1 requires a properly folded EGF domain as a substrate. *O*-fucosylation then occurs at a single unique residue, within a loose consensus sequence.[83-87] The first indication of this process came after the observation that there is decreased expression of a Notch reporter gene in cells that are deficient in GDP-fucose, the substrate used by O-FucT-1.[88,89] It was subsequently demonstrated that mutation or knockdown of *Ofut1* in *Drosophila* results in complete loss of Notch signaling, with phenotypes as severe as those in mutants with completely absent Notch receptor.[90-92] In mice, *Pofut1* mutants phenocopy mutants for the only murine CSL gene,[93] or double mutants for the two murine presenilin genes,[94,95] which are required for the proteolytic processing of Notch and subsequent NICD release.

Interestingly, the mouse *Pofut1* mutant phenotype is more severe than the phenotype observed for single *Notch* mutants (mouse has four different types of Notch receptors), indirectly indicating that *O*-fucosylation is required for the function of all Notch receptors. Detailed phenotypic analysis has also shown that *O*-fucosylation is required for all three main modes of Notch signaling: lateral inhibition, cell-lineage decision and inductive signaling. Finally, rather than simply being a permissive factor that is required for proper Notch signaling, recent evidence suggests that regulation of the distribution of O-FucT-1 controls the pattern of Notch activation. Even though both the *Drosophila Ofut1* gene and the murine *Pofut1* gene are broadly expressed, the mRNA transcripts are tightly regulated both spatially and temporally.[84,90,96] Ectopic expression *Ofut1* in *Drosophila* and *OFUT1* in cell culture has been observed to have both positive and negative effects Notch signaling, indicating that transcriptional regulation of *Ofut1* itself modulates Notch signaling.[90-92]

Following the addition of *O*-fucose to an EGF domain on Notch, the monosaccharide can be elongated to a disaccharide by Fringe. Initial evidence that Fringe may be involved in the synthesis of *O*-glycans on Notch came from observations that 1) bioinformatically, there is a weak similarity between Fringe and a bacterial galactosyltransferase, lex-1,[97] 2) Fringe influences the Notch pathway,[98-100] and 3) Notch contains consensus sequences for *O*-glycan modifications.[82,101] Biochemical characterization confirmed that Fringe catalyzes the second step in the synthesis of the *O*-fucose tetrasaccharide found on Notch EGF domains by transferring a GlcNac onto fucose in a 1,3 linkage.[88,102] Fringe uses fucose-*O*-EGF as a substrate, and prior fucosylation of the EGF domain by O-FucT-1 is required for proper Fringe activity. Like O-FucT-1, Fringe also has a preference for specific EGF domains,[88,103] and can glycosylate both the Notch receptor and Notch ligands.[86,88,102] It contains a highly

conserved DXD motif that is known to be essential for enzymatic activity in other glycosyltransferases.[104] Mutation of this motif eliminates the enzymatic activity of Fringe both in vivo and in vitro.[88,89,102,105] The ability of Fringe to influence Notch signaling is impaired in cells that are deficient in the synthesis of fucose-containing glycans, indicating that Fringe requires a fucose substrate.[88,89] Mutation of the gene *fringe connection*, which encodes a transporter for UDP-GlcNAc, the Fringe donor sugar, phenocopies fringe mutants.[106,107] This data conclusively demonstrates that Fringe is a glycosyltransferase that influences Notch signaling.

Fringe activity is both ligand and receptor specific. In general, Fringe acts as a positive regulator of Delta signaling and a negative regulator of Serrate/Jagged signaling, although there are exceptions that have been found in human cell culture experiments. In the *Drosophila* wing, Fringe potentiates the ability of Delta to activate Notch,[98] and at the same time inhibits the ability of Serrate to activate Notch.[98-100] Similarly, in cultured human tissue cells, Lunatic Fringe increases the signaling from Delta1 to Notch1,[108] and decreases the signaling from Jagged1 to Notch1.[88,89,108] However, Lunatic Fringe has been reported to potentiate the signaling of both Delta1 and Jagged1 to Notch2,[108] while another study reported decreased signaling by Jagged1 to Notch2, and no effect of Delta1 signaling to Notch2.[109]

Unlike O-FucT-1 activity, which is required for all three major modes of Notch signaling (lateral inhibition, cell-lineage decision and inductive signaling), Fringe appears to only affect inductive signaling.[100,110] This is best illustrated by its effects on Drosophila wing development, where Fringe creates a stripe of Notch signaling at the border of the anterior and posterior wing through opposing effects on Delta and Serrate.[51,111]

Even though *O*-linked glycans exert their influence on Notch activation at the cell surface, the actual act of glycosylation occurs in the Golgi. This is supported by two lines of evidence. First, a chimeric version of Fringe that is retained in the Golgi acts normally[102] while a secreted form has no activity, and second, the nucleoside sugar donors like GDP-fucose or UDP-GlcNAc are synthesized in the cytoplasm and then transported into the Gogli by transporters such as Fringe connection.[106,107] As a result, the extracellular concentration of the nucleoside sugar donors is too low to support glycosylation of Notch in its transmembrane location.

I.10. *Notch involvement in LR development*

Notch appears to be involved in the regulation of several keys steps of the LR developmental cascade. To date Notch has been implicated in LRO morphogenesis, LRO ciliary length control, symmetric peri-LRO *Nodal* expression, asymmetric *Nodal* expression at the left LPM, and asymmetric *PitX2* expression at the left LPM.

In mouse, concomitant loss of Dll1 and Baf60c, which binds to CSL and recruits the CSL co-activator complex, leads to disruption of the organization of the node.[112-114] In zebrafish, increased Notch signaling by overexpression of *NotchICD* and *deltaD* resulted in longer cilia via foxj1a.[115] Alternatively, decreased Notch signaling using mutant *deltaD*, a homologue of *Dll1*, led to shorter cilia and slow fluid flow in the LRO. However, *Dll1* null mice have been shown to have normal leftward LRO fluid flow.[112] Thus, the role of Notch signaling in LRO ciliogenesis and ciliary length control remains unclear.

In mice, *Dll1* or *Notch1*/*Notch2* double mutants have defects in laterality secondary to suppression of symmetric peri-LRO *Nodal* expression.[112,114,116] Symmetrically expressed

Nodal at the periphery of the LRO is required for left specific *Nodal* expression at the LPM.[117,118] There are two specific enhancers for *Nodal* expression. Symmetric peri-LRO *Nodal* expression is regulated by an enhancer in the upstream region of the *Nodal* gene, while left-sided LPM *Nodal* expression is regulated by an enhancer of *Nodal* found within intron 1.[119,120] The LRO specific enhancer contains two CSL-binding sites, which are functionally important for peri-LRO *Nodal* expression.[112,116] Additionally, Peri-LRO *Nodal* expression was also not detected in RBPjk (CSL) deficient mice.[116] Similar results have been obtained in zebrafish[116] and *Xenopus*.[121]

In zebrafish, expression of *cyclops* and *spaw*, two Nodal-related genes, at the left LPM is regulated by Notch signaling, although it appears that the two genes are regulated by different mechanisms. Increase in Notch signaling resulted in randomized expression of both genes at the LPM, but increased peri-LRO expression only for *Cyclops*.[116,122] Alternatively, decrease in Notch signaling by a ɣ-secretase inhibitor suppressed the expression of *charon*, a Cerebrus/Dan family member responsible for blocking transfer of spaw from the LRO to the right LPM.[42,123] As a result, lack of *charon* led to randomization of *Nodal* expression at the LPM.[122]

Dll1 has been reported to be asymmetrically expressed in chick, but not in other vertebrates, including mice and *Xenopus*.[112,121,124] Asymmetric Dll1 expression, and subsequent asymmetric *Nodal* expression is inhibited with omeprazole, a pharmacologic inhibitor of H^+/K^+-ATPase, indicating that H^+/K^+-ATPase activity could be responsible for asymmetric regulation of Notch signaling and LR axis formation in the chick LRO.[124] To date no LRO flow has been detected in the chick. Given that asymmetric Dll1 expression appears to be unique to the chick, it is plausible that the chick LR developmental cascade

may have diverged from that of other vertebrate model organisms, with Notch signaling providing a unique mode of LR axis formation.

Finally, in *Xenopus* Notch signaling has recently been implicated in *PitX2* expression at the LPM through the action of the transcriptional repressor B-cell lymphoma 6 (BCL6) and its co-repressor BCL6 co-repressor (BCoR).[121] Repression of Notch signaling by BCL6 and BCoR is required to allow *PitX2* expression at the left LPM. Knockdown of either BCL6 and BCoR resulted in abnormal heart looping, abnormal *PitX2* expression at the LPM, but normal expression of *Xnr1*, a homologue of *Nodal*, at the left LPM.

Altogether, there is convincing evidence that Notch signaling is involved in the regulation of peri-LRO expression of *Nodal*, and asymmetric expression of *PitX2* at the left LPM. However, there is conflicting evidence from different model organisms whether Notch signaling is involved in LR axis development via asymmetric Dll1 expression, or whether it is involved in the regulation LRO ciliary length, and left specific expression of *Nodal* at the LPM. In my work, I identify yet another mechanism for notch signaling at the LRO which unites ciliary cell fate, ciliary flow, and asymmetric nodal activation providing a simple mechanism for the relation between notch signaling and nodal activation. I obtained this result by the analysis of a novel gene, *Galnt11*, identified from a patient with heterotaxy, that has an important new role in notch signaling.

I.11. *Genetics of heterotaxy*

The genetics of human heterotaxy is characterized by two salient features: a high degree of locus heterogeneity combined with tremendous phenotypic variability.[2] In addition, the complexity of the associated heart disease results in a high degree of lethality

prior to reproductive age, thus limiting the number of extended pedigrees.[125,126] Familial cases of heterotaxy have shown tremendous phenotypic variability within many heterotaxy pedigrees, with the co-existence of situs solitus, situs inversus and isomerism syndromes within one family. Although these features complicate attempts to delineate the genetic contributions to heterotaxy, the wealth of gene information gleaned from studies of left-right development in model organism systems provides a singular opportunity to dissect the underlying genetic etiology.

At the current time, gene mutations have been associated with 10-20% of cases of heterotaxy.[127,128] These can be divided into syndromes with a known genetic etiology that have heterotaxy as an associated feature and isolated heterotaxy cases with an identified single-gene mutation. Consistent with the prominent role cilia play in the development of LR asymmetry, syndromes associated with defects in cilia structure and function can manifest with heterotaxy as part of the clinical spectrum (Table 1).

Primary Ciliary Dyskinesia

The syndrome with the most prominent association with heterotaxy is Primary Ciliary Dyskinesia (PCD or Kartagener syndrome). PCD consists of sino-pulmonary disease, male infertility and a 50% incidence of abnormal cardiac situs.[34] A minimum of 6.5% of patients with PCD have intracardiac disease consistent with heterotaxy.[129] PCD is caused by mutations in genes affecting function of motile cilia in the airway, the sperm flagellum and the motile cilia found on the left-right organizer during development. At this time, defects in 12 distinct genes have been associated with PCD (Table 1), and the repertoire is increasing as genomic analysis of affected patients becomes more sophisticated. Inheritance is

predominantly recessive, although rare dominant and X-linked pedigrees have been identified.

Bardet-Biedl Syndrome

Bardet-Biedl syndrome is a rare genetic disorder characterized by renal and hepatic cystic disease, retinitis pigmentosa, polydactyly, developmental delay and obesity. The cardiac manifestation is rare and shows situs inversus. 14 BBS genes have been identified to date, and they all focus on biogenesis and function of the centriole upon which the cilium is built.

Other syndromes that have been classified as "ciliopathies" also include cardiac disease that is part of the heterotaxy spectrum.[130] These include Meckel-Gruber syndrome, Short-Rib Polydactyly Syndrome and Ellis-van Creveld Syndrome. Ellis-van Creveld syndrome is a skeletal dysplasia associated with a high incidence of common atrium and systemic and pulmonary venous anomalies that are frequently seen in the context of Htx. Mutations in two genes, EVC and EVC2 underlie approximately 70% of cases; EVC and EVC2 interact at the cilium to affect hedgehog signaling.[131] Dextrocardia has been seen in the context of VACTERL-H syndrome, and one possible molecular etiology for VACTERL-H is a deletion encompassing the Zic3 gene, which also causes X-linked non-syndromic heterotaxy.[132]

Table 1. List of syndromes involving heterotaxy and associated gene mutations

Syndrome	**Cardiac Disease**	**Other clinical Features**	**Gene(s) and References**	**Molecular/Cellular Ontology**
Primary Ciliary	Situs Inversus	Chronic sinusitis,	DNAI1,	Structure and function of

Dyskinesia (PCD)	Totalis (50%), Heterotaxy (6.5%)	bronchiectasis, neonatal respiratory distress, male infertility Occasional: female infertility, retinopathy	DNAI2, DNAH5, DNAH11, RSPH9, RSPH4A, LRRC50, RPGR, TXNDC3, KTU, CCDC40, CCDC39,	motile cilia
Bardet-Biedl Syndrome (BBS)	Rare situs inversus, up to 50% with minor cardiac abnormalities	Renal abnormalities, polydactyly, retinal dystrophy, hearing loss, obesity, developmental delay, hypogonadism,	BBS1,2,4,5,7-10,12 Arl6(BBS3) , TRIM32 (BBS11) , BBS14	Centriole/Basal body structure and function
Meckel-Gruber Syndrome	20% CHD including rare situs inversus	Encephalocele, polydactyly, polycystic kidneys, hepatic abnormalities	MKS1, TMEM216 (MKS2), TMEM67 (MKS3),	Primary Cilium and basal body

			RPGRIP1L, CC2D2A	
Nephronopthisis	Situs inversus, VSD	Cystic kidney disease, retinal degeneration	NPHP1, INVS (NPHP2), NPHP3, NPHP4, NPHP5, CEP290, (NPHP6), GLIS2, (NPHP7) , NEK8 (NPHP8)	Cilium, Centriole, Cell cycle
VACTERL-H	VSD, Dextrocardia (rare)	Vertebral anomalies, anal atresia, tracheoesophageal fistula, limb abnormalities, hydrocephalus, renal hypoplasia	Zic3	Unknown
Ellis-Van-Creveld Syndrome	Atrio-venytricular canal,	Short ribs, polydactylay, ectodermal	EVC1, EVC2	Hedgehog signaling, cilium

	Common Atrium, LSVC	dysplasia, renal abnormalities		

I.12. ***Non-syndromic heterotaxy and the role of CNVs in causative heterotaxy genes***

A major limitation in identifying causative genes in heterotaxy is the paucity of families segregating highly penetrant alleles, and the high locus heterogeneity, which has limited the ability to map disease loci. Because of marked impairment in reproductive fitness, some fraction of heterotaxy could be caused by very rare, highly penetrant, dominant mutations. Although such mutations have historically been difficult to identify, recent advances have improved the ability to detect these. For example, the use of quantitative interrogation of dense sets of SNPs has dramatically improved the ability to detect small copy number variants (CNVs). The significance of such rare mutations can be difficult to establish in the setting of high locus heterogeneity, as is the case for heterotaxy, where discovering a second hit in the same gene in a small cohort is unlikely.

This obstacle has recently been overcome by using *X. tropicalis* as a high-throughput model system to test the validity of rare genes identified through CNVs.[133] *X. tropicalis* has a mechanism of LR development that is highly conserved throughout vertebrate species, can produce large numbers of embryos that complete asymmetric heart and gut looping in a short time frame (4-5 days), and has a relatively compact diploid genome that retains substantial synteny to human, simplifying the identification of orthologous genes.[12,15,134] High-resolution genotyping of 262 heterotaxy subjects and 991 controls revealed 38 small CNVs that

encompassed 61 genes, 38 of which have *X. tropicalis* orthologs (in the most recent genome assembly, 22 in the previous genome assembly). 7 genes had favorable in situ expression patterns in ciliated organs and/or the heart, and 5 of them affected LR development when knocked down with MO. One of the five genes identified was *Galnt11*, a putative glycosylation factor that has not been characterized previously.[133]

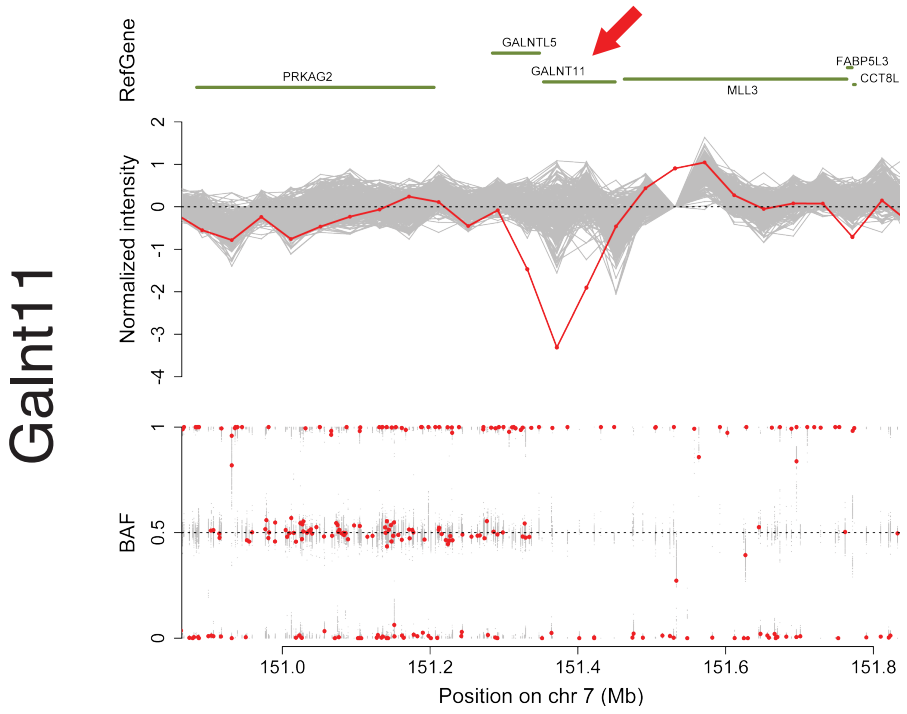

Figure 6. Deletion of Galnt11 in a patient with heterotaxy. Genes located in the segment are shown at the top, followed by the results of Illumina genotyping in the middle, and qPCR at the bottom of the figure. Both genotyping and qPCR results indicate a deletion in the first 3 exons of GALNT11.

I.13. *Galnt11*

Galnt11 is part of a family of twenty distinct GalNAc-transferases (Galnts), which play an essential role in *O*-GalNAc glycosylation in eukaryotes. O-GalNAc glycosylation is found on more than 10% of human proteins and more than 50% of the proteins passing through the secretory pathway.[135,136] This process of *O*-GalNAc sugar chain addition to

proteins is catalyzed by a complex set of enzymes localized at the Golgi apparatus.[137,138] The Galnt family catalyzes the first step of this cascade where they add a GalNAc residue onto Ser/Thr amino acids in proteins.[139,140] Following the addition of a GalNAc residue, different core-forming enzymes generate various core *O*-glycan structures, which can themselves then be further extended before being capped with histo-blood group-related structures or sialic acid.[141] Extensive *in vitro* studies have identified various substrates for Galnt enzymes. Members of the family appear to have different, but somewhat overlapping, substrate specificity.[141,142] However, direct *in vivo* protein targets have only been identified for several Galnt enzymes. In humans, Galnt3 is required for O-glycosylation of a specific site in fibroblast growth factor 23 (FGF23) that prevents proprotein convertase inactivation of FGF23, and loss of Galnt3 function leads to familial tumoral calcinosis.[143,144] Galnt2 appears to *O*-glycosylate a specific proprotein convertase site in angiopoietin-like protein 3 that is involved in in maintaining normal levels of plasma lipids.[145-148] In mice, Galnt1 is necessary for *O*-glycosylation of osteopontin and bone sialoprotein.[149] Finally, in *Drosophila* Galnt3 is important for *O*-glycosylation of the integrin-binding ligand tiggrin, which plays an essential role in the adhesion of dorsal and ventral cell layers in the basal matrix of the Drosophila wing.[150] However, to the best of our knowledge, to date there have been no *in vivo* protein targets identified for Galnt11.

I set out to discover the function of Galnt11 in LR patterning. Prior to my studies, we knew that Galnt11 was strongly expressed in the kidney (a ciliated structure) and that knockdown of Galnt11 led to LR defects recapitulating the human disease, heterotaxy. However, other than sequence relation to a family of GalNAc-transferases no functional role

for Galnt11 had been identified, the mechanism of Galnt11 in LR patterning was unknown, and no known targets of galnt11 had been identified.

II. HYPOTHESIS

Galnt11 is a GalNAc-transferase that is necessary for proper left-right axis establishment and heart looping. Its function is to specify between motile and sensory cell fates at the Left-Right Organizer by glycosylating Notch receptor and modifying Notch signaling.

III. METHODS

III.1. *In vitro fertilization and embryo injection*

In vitro fertilization was performed according to Khokha et al.[151] Briefly, male and female frogs were primed with 20 units of human chorionic gonadotropin (hCG; Chorulon) 12-36 hours before IVF. A boosting dose of 200 units hCG was injected 3–4 hours before IVF. Crushed male testes and female eggs were mixed in dishes coated with standard 1x MBS solution with 0.1% bovine serum albumin (BSA), and subsequently allowed to fertilize in 0.1x MBS solution (pH = 7.8–8.0). Once fertilized, the one-cell embryos were de-jellied using 3% cysteine in 1/9x MR (pH = 7.8–8.0), washed with 0.1x MBS, and put at 20 °C in a 3% Ficoll in 1/9x MR solution to retard the cell division process.

Embryos were injected at the 1- and 2-cell stage using an Narishige microinjection apparatus. Drop size was calibrated to 8nl per injection using micrometers to measure diameter of droplet. Injection doses for both MO and RNA were titrated to minimize toxicity. Following injection, embryos were allowed to rest for one hour at room temperature. Normally dividing embryos were then sorted and allowed to develop in 1/9x MR with 1x gentamycin (100 µg/ml) at 22-28 °C, depending on desired development rate.

III.2. *MO design*

Morpholino oligonucleotides were designed against the start and splice site of *X. tropicalis* Galnt11 (start site MO sequence 5’ to 3’: GCGCTGCCCATCGTCCCCCTAGCA T; splice site MO sequence 5’ to 3’: AGTAGGTGCCCTTCTCTCTGACCTG), as well as against the start site of *X. tropicalis* Notch1 (sequence 5’ to 3’: GAACAAGCAGCCCGATC CGATACAT).

III.3. *Heart looping scoring*

Following injection of MO or RNA, *X. tropicalis* embryos were incubated at 28 °C until they reached Nieuwkoop and Faber (NF) stage 45. Tadpole hearts were scored as either D-looped, for normal outflow tract looping from right to left, L-looped, for mirror image looping from left to right, or A-looped, for hearts that lacked either D- or L-looping (Figure).

III.4. *GRP dissection*

Neurula stage *X. tropicalis* embryos were used to dissect the GRP according to Blum et al.[15] All dissections were performed in 0.1x MBSH in agarose-coated plates. A transverse cut perpendicular to the AP plane was used to open the embryo. At this point the gastrocoel cavity was visualized, with the neural folds being positioned dorsally, and located ventrally. The left and right edges of the gastocoel cavity were then dissected towards the posterior tip of the embryo until the two dissection planes met and the ventral yolk side was removed.

III.5. *In situ hybridization*

Whole mount embryos and dissected GRPs were fixed in MEMFA for 1-2 hours. If LacZ/RedGal staining was used, embryos were fixed in MEMFA for 1 hour, followed by staining in RedGal mix (variable time, until red stain appears), followed by re-fixation with MEMFA for 1 hour. Digoxigenin-labeled (Roche) RNA probes were prepared from linearized plasmids using SP6 or T7 RNA polymerase (Ambion, NEB respectively) We used a standard *X. tropicalis* whole-mount in situ hybridization protocol.

III.6. ***Immunohistochemistry***

Whole mount embryos and dissected GRPs were fixed in 4% paraformaldehyde (PFA) in 1x PBT solution for 1 hour, followed by cold ethanol fixation at 4 °C for 4 hours. If the embryos had been injected with GFP or RFP, they were fixed in 4% PFA in 1x PBT solution for 4 hour with no cold ethanol fixation. Primary antibodies used were mouse monoclonal antibody directed against acetylated alpha tubulin (1:1000; Sigma), mouse monoclonal antibody directed against Galnt11 (1:1).[139]

Fixed embryos and GRPs were permeabilized with 0.2% Triton in PBS (PBT), blocked in 2% BSA in PBT, and subsequently incubated with primary antibodies and Texas red- and Alexa Fluor 488-conjugated secondary antibodies (Invitrogen). Embryos were mounted in Pro-long antifade (Invitrogen) and imaged on a Zeiss Axioskop.

III.7. ***Electron microscopy***

Whole mount embryos and dissected GRPs were quickly washed in 1x PBS (Ca2+ free) with 1mM EDTA and fixed in 2.5% glutaraldehyde, 50mM Hepes, 2mM MgI and 1mM EDTA for one hour at room temperature, followed by one hour at 4 °C. The samples were then washed with 50mM Hepes and delivered to the Yale Electron Microscopy Laboratory for further processing.

III.8. ***Video-tracking of tadpoles***

Embryos were unilaterally injected at the 2-cell stage with 1.0ng *Galnt11* MO and Alexa Fluor 488 lineage tracer (Invitrogen). Specimens were raised to stage 32 in 1/9x MR + Gentamycin. To circumvent muscle contractions (active swimming), which would

compromise cilia-based motion, embryos were anesthetized with benzocaine. After validation of unilateral lineage tracer expression, embryos were placed individually in agarose-coated Petri dishes with 1/9x MR + benzocaine. Embryo motion was recorded for 10 min at 0.1 fps using a Canon EOS 5D MarkII and DSLR Remote Pro 1.3 (Breeze Systems). Subsequently, each embryo was flipped over to the other side and motion was similarly recorded. Movies were analyzed using ImageJ (NIH). Individual images were superimposed onto each other to create a path line that was used to calculate the total distance travelled. Embryos which showed no movement or movement that was interrupted artificially (e.g. caused by unevenness of the agarose) were excluded from the analysis. The uninjected side served as internal control. Determination of statistical significance was performed by Wilcoxon matched pairs test (Microsoft Excel).

III.9. *Roles*

All work presented in this thesis was performed by the author, Marko T. Boskovski.

IV. RESULTS

IV.1. *Galnt11 is required for proper heart looping*

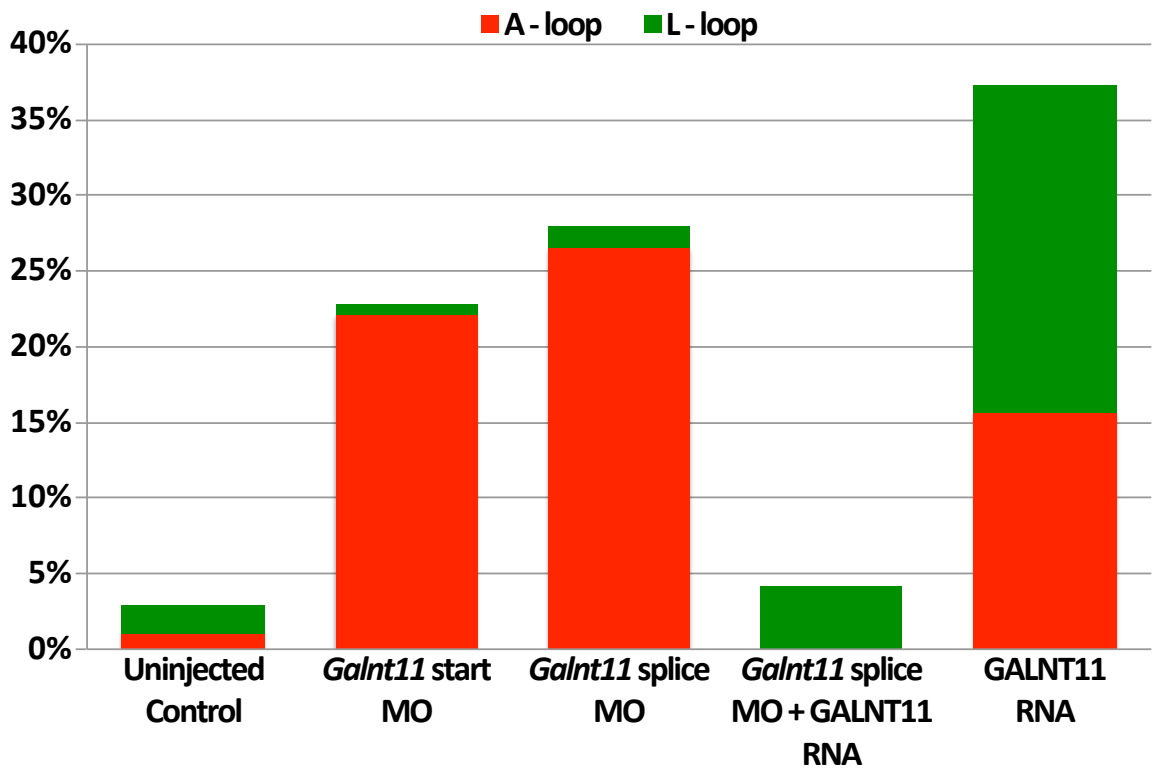

Figure 7. Knockdown of *Galnt11* with a start- and splice-site MO results in a significant number of looping abnormalities, compared to uninjected control. These looping abnormalities can be rescued by coinjection of *Galnt11* splice-site MO and human GALNT11 RNA. Overexpression with GALNT11 RNA also produces abnormal looping.

To determine whether knockdown or overexpression of *Galnt11* affects proper LR axis formation, we injected a start-site *Galnt11* MO, a splice-site *Galnt11* MO and GALNT11 RNA at the one-cell stage, and examined the resulting embryos for heart looping defects at NF stage 45. Uninjected control embryos had 2.9% looping abnormalities (1.1% A-loops and 1.8% L-loops, n = 252). By contrast, start-site *Galnt11* MO injected embryos had 22.8% looping abnormalities (22.1% A-loops and 0.7% L-loops, n = 145), splice-site *Galnt11* MO injected embryos had 27.9% looping abnormalities (26.5% A-loops and 1.5%

L-loops, n = 223), and GALNT11 RNA injected embryos had 37.3% looping abnormalities (15.7% A-loops and 21.6% L-loops, n = 187) (Fig. 6). This suggests that a very specific dose of Galnt11 transcript is required for proper LR axis development, and that either knockdown or overexpression leads to heart looping defects.

IV.2. *Galnt11 MO induced heart looping defects can be rescued with human GALNT11 RNA*

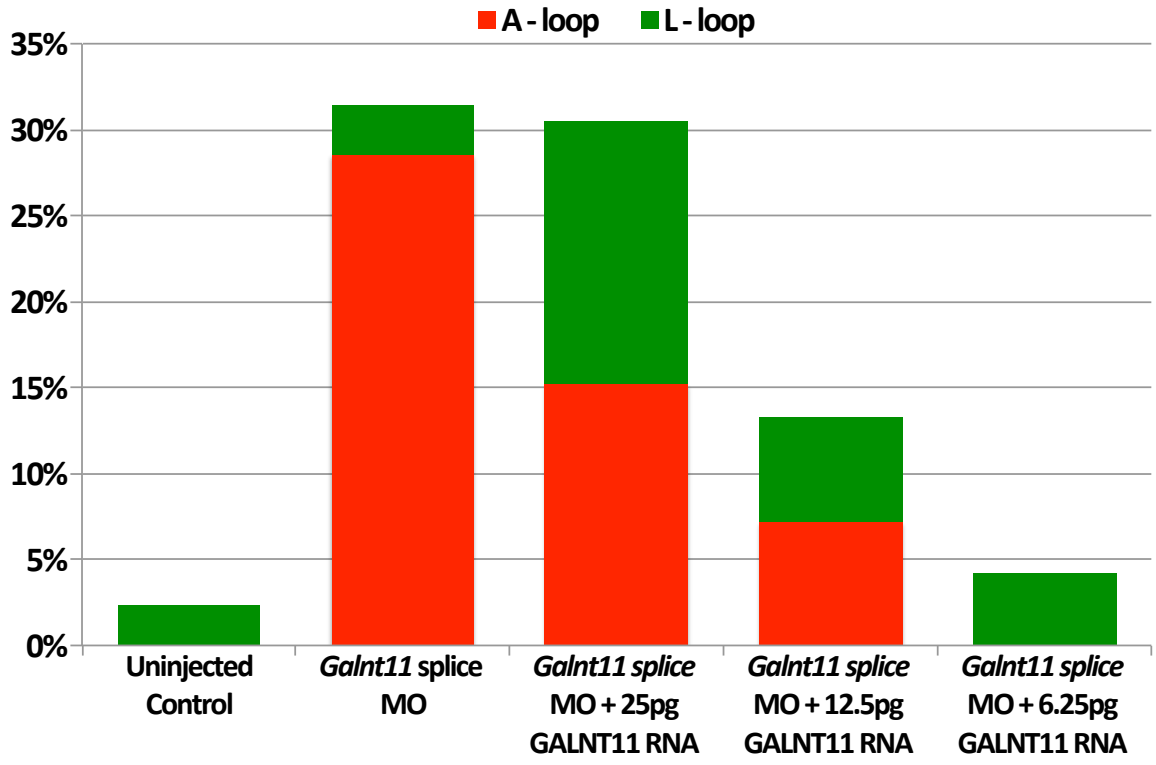

Figure 8. Looping abnormalities induced by *Galnt11* MO can be rescued with human GALNT11 RNA in a dose dependent fashion.

The similarity in phenotypes between the start- and splice-site *Galnt11* MOs suggested that both MOs are specific. To test this more rigorously, we attempted to rescue the *Galnt11* splice-site MO with a human GALNT11 RNA construct by injecting a constant

dose of 0.5ng of MO and titrating the GALNT11 RNA dose. Compared to 31.4% looping defects (26.5% A-loops and 1.5% L-loops, n = 93) after injection of *Galnt11* MO only, co-injection of *Galnt11* MO with 25pg of GALNT11 RNA resulted in 30.4% looping defects (15.2% A-loops and 15.2% L-loops, n = 96), co-injection of *Galnt11* MO with 12.5pg of GALNT11 RNA resulted in 13.3% looping defects (7.2% A-loops and 6.0% L-loops, n = 119), and co-injection of *Galnt11* MO with 6.25pg of GALNT11 RNA resulted in 4.2% looping defects (0% A-loops and 4.2% L-loops, n = 103) (Fig. 7). This demonstrates that the splice-site *Galnt11* MO is specific and can be rescued in *X. tropicalis* with a human GALNT11 construct. All other experiments requiring knockdown of *Galnt11* were performed using the *Galnt11* splice-site MO.

IV.3. *Galnt11 affects Coco and PitX2 expression*

To test where along the LR axis developmental pathway Galnt11 acts, we looked to see if abnormal levels of *Galnt11* lead to abnormal *Coco or PitX2* expression patterns using whole mount in situ hybridization. *Coco* is the earliest asymmetrically expressed gene in the LR cascade where the right side has stronger expression than the left, and *PitX2* is the last asymmetrically expressed gene before asymmetric organogenesis. *PitX2* is normally expressed at the left LPM and not the right. As expected uninjected control embryos had only 4.5% abnormal *PitX2* expression (0% expression on the right side only; 2.2% absent expression on either side; 2.2% bilateral expression, n = 69) (Fig. 8). However, *Galnt11* MO injected embryos had 22.2% abnormal *PitX2* expression (0% right side only; 14.8% absent; 7.4% bilateral, n = 64), and GALNT11 RNA injected embryos had 29.4% abnormal *PitX2*

expression (8.8% right side only; 2.9% absent; 17.6% bilateral, n = 69), indicating that Galnt11 acts upstream of *PitX2*.

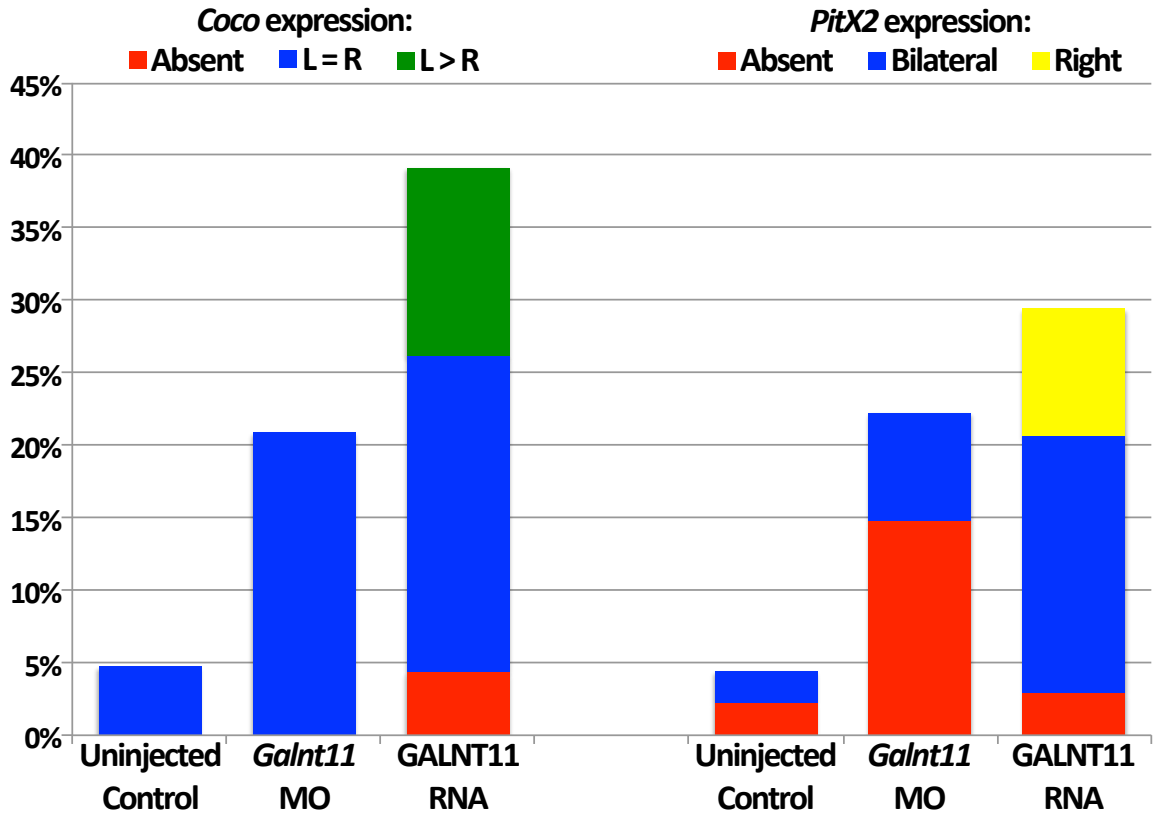

Figure 9. Both *Galnt11* MO and GALNT11 RNA yield abnormal *Coco* and *PitX2* expression patterns.

For *Coco* expression, GRPs from uninjected control embryos also had low percentage of abnormal expression (95.2% right greater than left; 4.8% right equal to left; 0% left greater than right; 0% no expression, n = 33). *Galnt11* MO injected embryos had 20.9% abnormal *Coco* expression (20.8% R = L; 0% L > R; 0% no expression, n = 32), and GALNT11 RNA injected embryos had 39.1% abnormal *Coco* expression (21.7% R = L; 13.0% L > R; 4.3% no expression, n = 37), indicating that Galnt11 also acts upstream of *Coco*. Since *Coco* is asymmetrically expressed in direct response to LRO flow, abnormal

Coco expression in the presence of abnormal Galnt11 levels suggests that Galnt11 is involved either in the process of flow generation or flow sensation.

IV.4. *Galnt11 is expressed in the X. tropicalis GRP and kidneys, and Galnt11 protein is present in the mouse node*

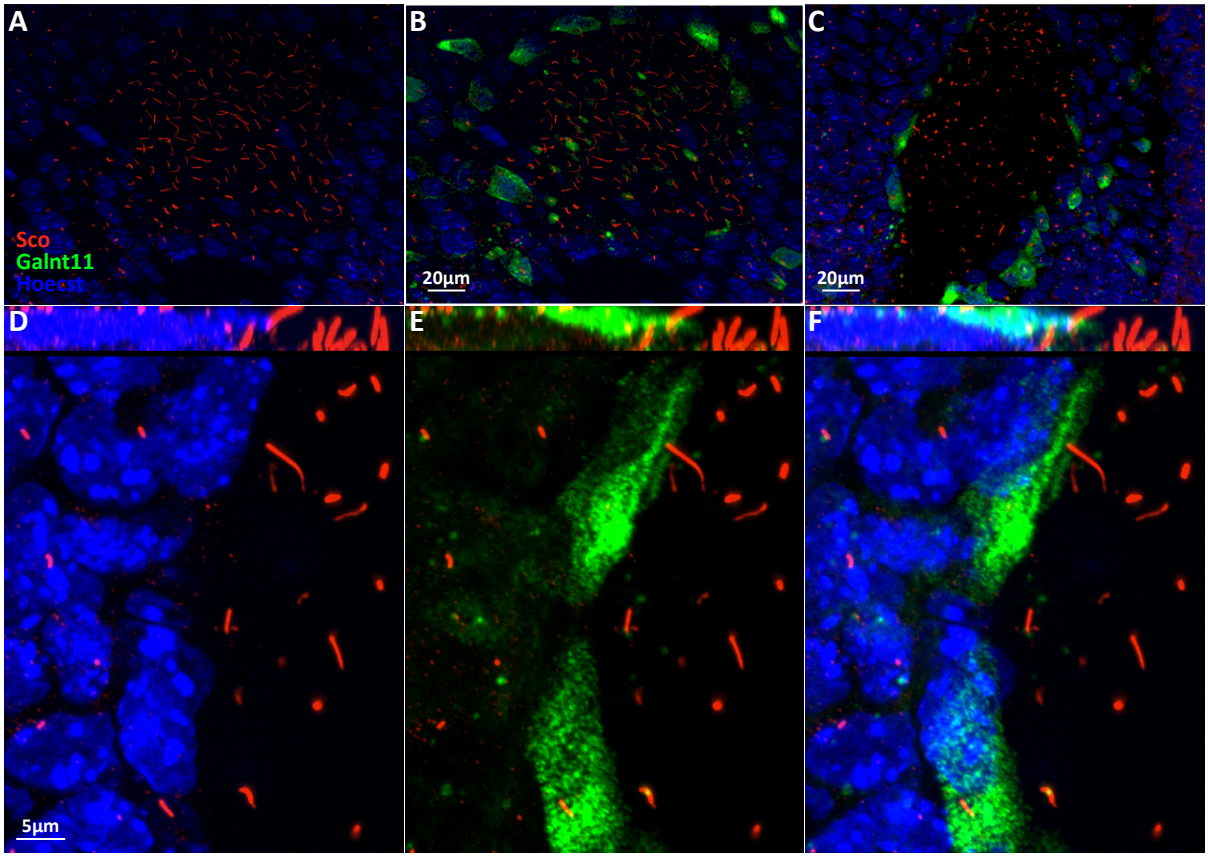

Figure 10. Immunofluorescence pictures demonstrating that Galnt11 localizes to the crown cells surrounding the pit cells in the LRO. **A.** The mouse LRO with cilia in red and no Galnt11. **B and C.** The mouse LRO with cilia in red and Galnt11 in green. **D-F.** Close up of the border between the crown and pit cells where Galnt11 localizes.

Given that Galnt11 appears to be acting at the level of the LRO where asymmetric flow is created and sensed, we hypothesized that *Galnt11* would be expressed during *X. tropicalis* stages 14 – 20 when the LRO cilia form and start functioning to break LR asymmetry. Whole mount and GRP in situ hybridization of wild type embryos during these

stages revealed strong *Galnt11* expression during stages. Interestingly, during later stages *Galnt11* was also strongly expressed in the kidneys, which is another ciliated organ like the LRO. We also used a mouse monoclonal antibody against Galnt11 in E8.0 mouse embryos. Galnt11 protein was strongly present in the crown cells surrounding the pit cells of the LRO (Fig. 9), further suggesting that Galnt11 affects LRO cilia.

IV.5. *Galnt11 is only required on the left side for proper heart looping*

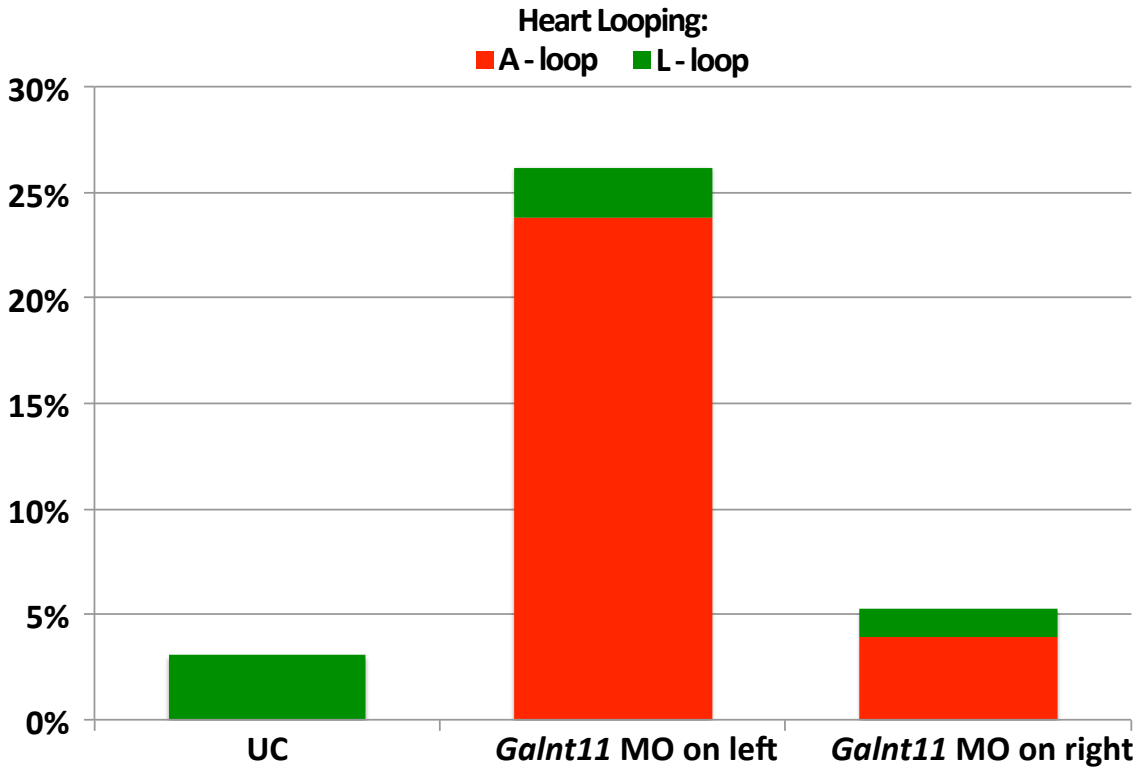

Figure 11. Only injection of *Galnt11* MO on the left produces heart looping defects.

To further investigate the role of Galnt11 in LR axis formation, we exploited an experimentally useful property of *Xenopus* – at the two-cell stage, one of the two cells approximates the left side of the developing tadpole, while the other cell approximates the right side. This allowed us to test whether Galnt11 is required on the left, right, or both sides

for proper heart looping. When we injected *Galnt11* MO on the right there were 26.2% heart looping defects (23.8% A-loop, 2.4% L-loop, n = 144), while when we injected *Galnt11* MO on the left there were 5.3% heart looping defects (3.9% A-loop, 1.3% L-loop, n =121) (Fig. 10), indicating that Galnt11 is only required on the left side for proper heart looping.

IV.6. *Galnt11 does not appear to affect the ultrastructure of epidermal cilia*

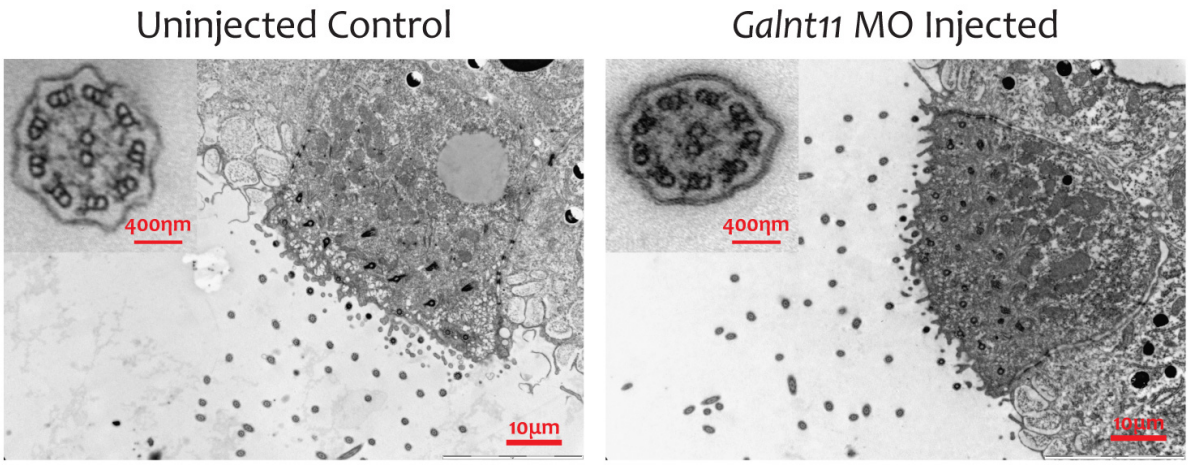

Figure 12. Transmission electron microscope images of uninjected control and *Galnt11* morphant embryos reveal no differences in ciliary ultrastructure.

Since *Galnt11* is strongly expressed in ciliated organs like the GRP and the kidneys, we wondered whether knockdown of *Galnt11* would lead to abnormalities in the ultrastructure of cilia which we can study with electron microscopy. The epidermis of *X. tropicalis* is ciliated, with several hundred cilia present on ciliated epidermal cells interspersed relatively evenly among non-ciliated epidermal cells. Scanning electron microscopy revealed no differences between cilia clumps on uninjected control embryos and those injected with *Galnt11* MO. Transmission electron microscopy also revealed no differences, and cilia on *Galnt11* MO injected embryos had a normal arrangement of nine microtubule pairs with outer and inner dynein arms, and a central microtubule pair in the

middle (Fig. 11). However, lower magnification SEM images suggested that the cilia clump density of *Galnt11* MO injected embryos might be higher than that of uninjected control embryos.

IV.7. *Galnt11 and Notch1 affect epidermal cilia density*

To more closely evaluate whether *Galnt11* influences cilia-clump density at the epidermis, we again performed two-cell injections with *Galnt11* MO or GALNT11 RNA, and compared the injected side with the uninjected. GFP was co-injected as a tracer, and the cilia were labeled fluorescently with anti-acetylated tubulin antibody. Similar to our observations with EM, the *Galnt11* MO injected side appeared to have an increased cilia-clump density compared to the uninjected side. Conversely, injection of GALNT11 RNA on one side significantly decreased the cilia-clump density compared to control (Fig. 12).

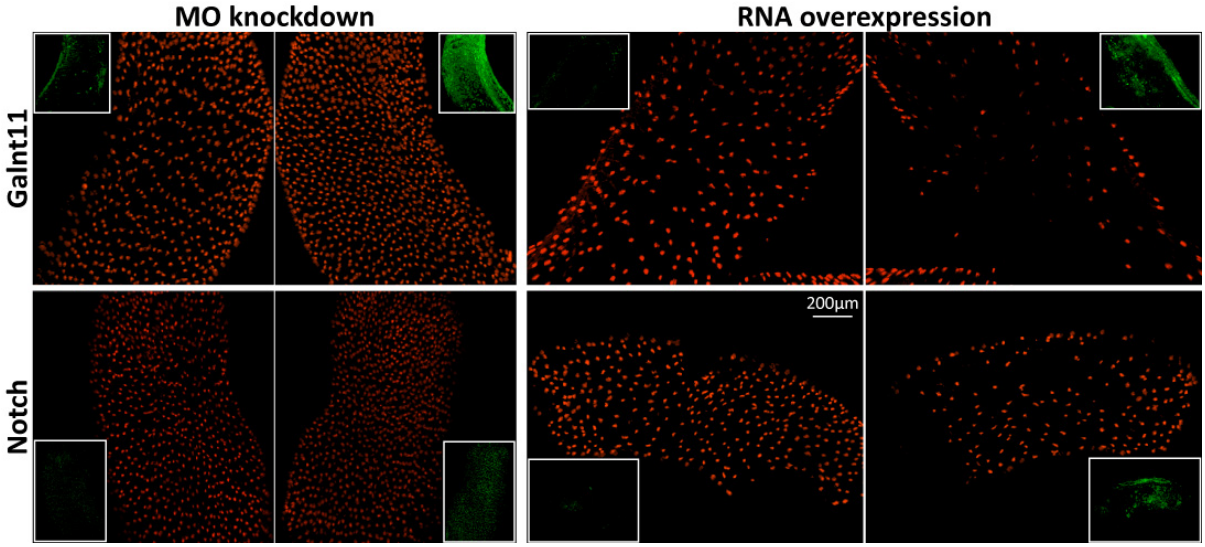

Figure 13. Immunofluorescence pictures illustrating that Galnt11 and Notch affect the epidermal cilia clump density in a similar manner. On the left, knockdown of either *Galnt11* or *Notch1* produces an increase in cilia clump density, while on the right, overexpression of either *Galnt11* or *Notch1* results in a decrease in cilia clump density. Acetylated tubulin marks cilia in red, and GFP in green marks the embryo side that was injected.

There is an extensive literature that epidermal cilia density is regulated by Notch signaling. Indeed, similar to our Galnt11 results, cilia-clump density increased when we injected *Notch1* MO, and decreased when we injected *Notch ICD*, which constitutively activates the Notch pathway. These results suggest that Galnt11 and Notch either interact or act in parallel pathways to affect cilia-clump density.

IV.8. *Galnt11 affects cilia driven embryo gliding*

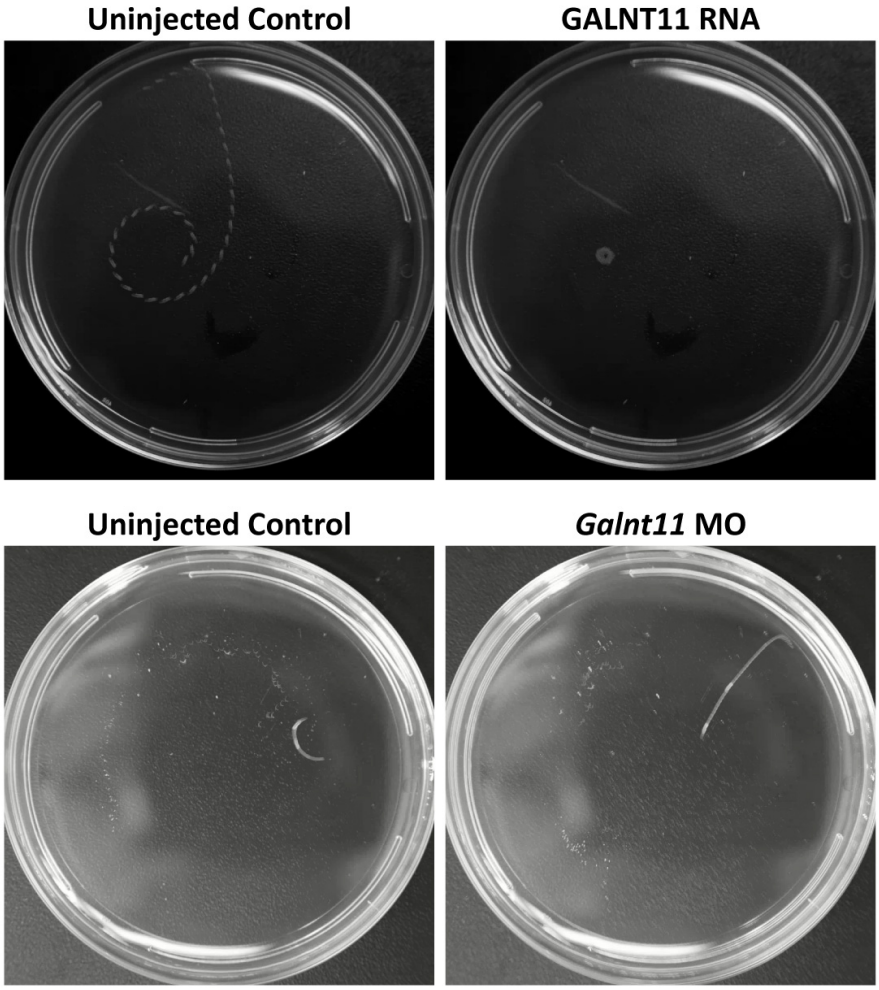

Figure 14. Composite images of tadpole epidermal cilia gliding videos. Tadpole gliding over a fixed time period can be seen as a white line. Overexpression with GALNT11 RNA retards ciliary gliding, while knockdown with *Galnt11* MO significantly speeds it up.

Given that Galnt11 affects cilia-clump density, we wondered whether manipulation of Galnt11 levels and cilia-clump density has any functional significance. To evaluate this, we used a tadpole-gliding assay originally devised by Vick et al., which evaluates the ability of epidermal cilia to propel an otherwise paralyzed tadpole across an agarose coated petri dish. Again, embryos were injected at the two-cell stage in identical fashion as when evaluating cilia density. When injected with *Galnt11* MO, the tadpoles glided significantly faster on the injected side compared to the uninjected side suggesting that at the very least the function of these cilia are normal. Conversely, when injected with GALNT11 RNA, the tadpoles glided significantly slower on the injected side compared to the uninjected side (Fig. 13). To be clear, glide speed seemed to relate inversely with the dose of Galnt11; higher doses of Galnt11 led to slower glide speeds which appeared to correlate nicely with cilia clump density. Thus, different levels of Galnt11 do not appear to affect the function of individual cilia, but do affect the ability of cilia clumps to collectively push fluid near the epidermis or propel the tadpole on a hard surface based on the number of cilia clumps present.

IV.9. *Galnt11 and Notch1 affect Coco and PitX2 expression and heart looping in a similar manner*

The epidermal results suggest that Galnt11 and Notch act in a similar manner. We examined this possibility further by comparing the effect of each gene on the LR developmental cascade, namely *Coco* and *PitX2* expression, as well as heart looping. MO knockdown of both *Galnt11* and *Notch1* yielded similar rates of heart looping defects that were significantly higher than uninjected controls (Fig. 14). UC embryos had 2.9% heart looping defects (1.1% A-loops, 1.8% L-loops, n = 112), compared with *Galnt11* morphants

which, had 28.0% heart looping defects (26.5% A-loops, 1.5% L-loops, n = 100) and *Notch1* morphants, which had 23.5% heart looping defects (20.6% A-loops, 2.9% L-loops, n = 103). Overexpression with GALNT11 RNA yielded 34.1% heart looping defects (17.6% A-loops, 16.5% L-loops, n = 104), and *NotchICD* RNA 28.0% heart looping defects (26.0% A-loops, 2.0% L-loops, n = 116), , indicating that the overall rate of heart looping defects is similar, but the proportion of A-loops vs. L-loops is different. GALNT11 overexpressed embryos had an almost equal number of A-loops and L-loops, while *Notch ICD* overexpressed embryos had mostly A-loops.

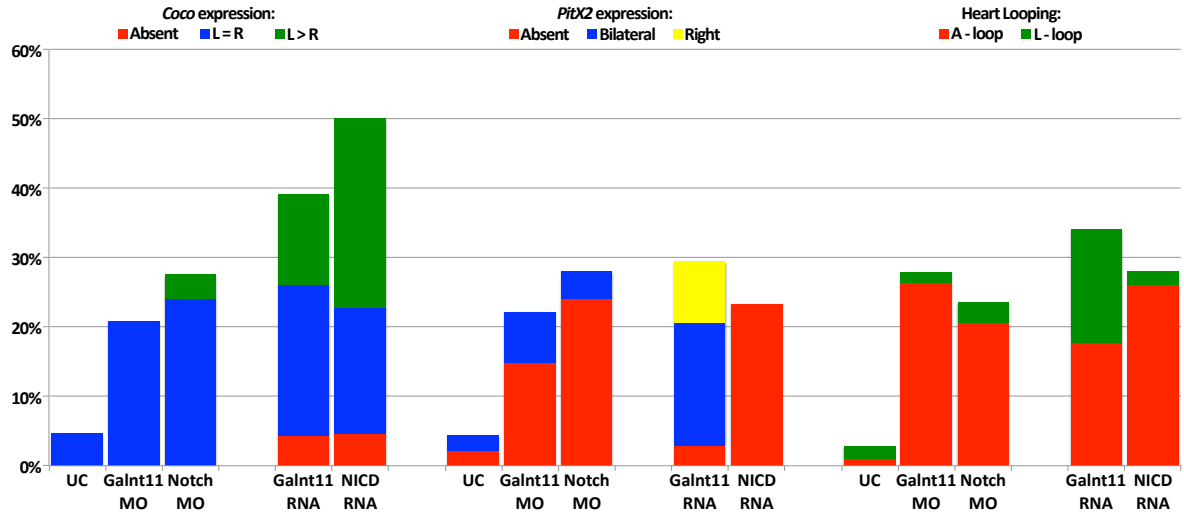

Figure 15. Galnt11 and Notch affect heart looping, as well as *Coco* and *PitX2* expression in a similar manner.

PitX2 expression at the LPM was also similarly affected by knockdown of *Galnt11* and *Notch1*. Compared to UC embryos which had 4.45% abnormal *PitX2* expression (0% right, 2.2% absent, 2.2% bilateral, n = 59), knockdown with *Galnt11* MO yielded abnormal *PitX2* expression in 22.2% of embryos (0% right, 14.8% absent, 7.4% bilateral, n = 50), while knockdown with *Notch1* MO yielded abnormal *PitX2* expression in 28% of embryos (0% right, 24.0% absent, 2.0% bilateral, n = 65). Overexpression with GALNT11 RNA and

NotchICD RNA yielded abnormal *PitX2* expression in 29.4% (8.8% right, 2.9% absent, 17.6% bilateral, n =68) and 23.3% (0% right, 23.3% absent, 0% bilateral, n = 72) of embryos, respectively. The *PitX2* expression patterns at the LPM parallel the heart looping patterns. Knockdown of either *Galnt11* or *Notch1* produces indistinguishable results with similar rates of right, absent and bilateral expression. However, while overexpression with GALNT11 and NICD RNA resulted in similar overall rates of abnormal *PitX2* expression, the relative ratios of right, absent and bilateral expression differed. GALNT11 overexpression resulted in mostly bilateral *PitX2* expression defects, with smaller numbers of absent and right expression. *Notch ICD* overexpression on the other hand only resulted in absent *PitX2* expression.

Coco expression at the GRP was similarly affected both by knockdown and overexpression of Galnt11 and Notch. UC GRPs had 4.8% abnormal *Coco* expression (4.8% R = L, 0% L > R, 0% absent, n = 35), compared with 21.8% abnormal *Coco* expression (21.8% R = L, 0% L > R, 0% absent, n = 43) for *Galnt11* MO injected GRPs, 27.6% abnormal *Coco* expression (24.1% R = L, 3.4% L > R, 0% absent, n = 45) for *Notch1* MO injected GRPs, 39.4% abnormal *Coco* expression (21.7% R = L, 13% L > R, 4.3% absent, n = 50) for GALNT11 RNA injected GRPs, AND 50.0% abnormal *Coco* expression (18.2% R = L, 27.3% L > R, 4.6% absent, n = 41) for NICD RNA injected GRPs. This suggests that both Galnt11 and Notch affect LR development upstream of *Coco* expression at the level of the ciliated GRP. Interestingly, there was no divergence in *Coco* expression phenotype with overexpression of Galnt11 and Notch as was seen with *PitX2* expression and heart looping.

IV.10. *Galnt11 MO can be rescued with Notch ICD and Su(H)-Ank, but not Delta*

Components of the Notch pathway, including Notch ligands and receptors are targets for glycosylation. While glycosylation of Notch ligands has an unknown role, glycosylation of Notch receptors acts to modify their sensitivity to ligand. Since Galnt11 is a galactosyltransferase with no known target protein to date, we hypothesized that Galnt11 glycosylates Notch receptor to modify Notch signaling. To test whether Galnt11 affects the function of Notch receptor we carried out a series of epistasis experiments.

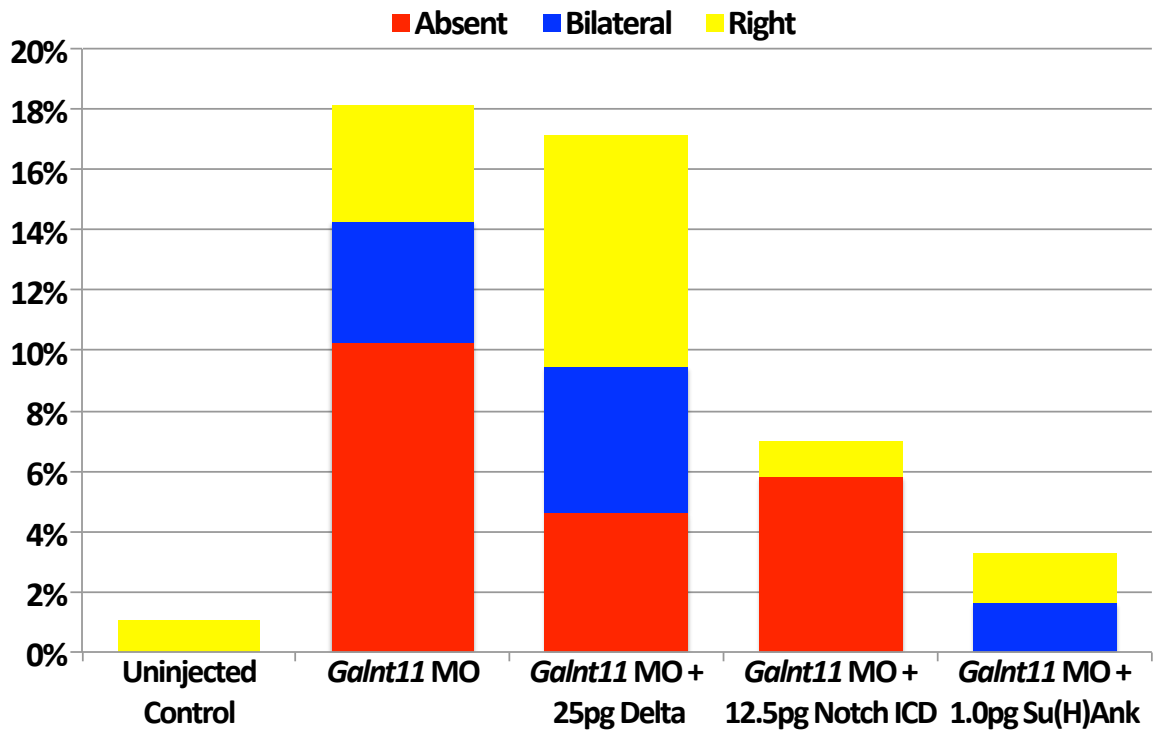

Figure 16. Abnormal *PitX2* expression at the LPM in *Galnt11* morphants can be rescued with *NotchICD* and *Su(H)-Ank*, but not *Delta.*

We injected one-cell embryos with *Galnt11* MO and evaluated for *PitX2* expression at the LPM. We then tried to rescue the abnormal *PitX2* expression patterns induced by *Galnt11* MO by injecting RNA constructs for one of three basic Notch components in one of two cells at the two-cell stage: *Delta*, *Notch ICD*, or *Su(H)-Ank* (Fig. 15). Positive control embryos that were only injected with *Galnt11* MO had 18.0% abnormal *PitX2* expression

(3.8% right, 10.3% absent, 4.0% bilateral, n = 76). When *Galnt11* MO rescue was attempted with *Delta* RNA there was 16.9% abnormal *PitX2* expression (7.7% right, 4.6% absent, 4.8% bilateral, n = 72). When *Galnt11* MO rescue was attempted with *Notch ICD* RNA there was 7.0% abnormal *PitX2* expression (1.2% right, 5.8% absent, 0% bilateral, n = 69). When *Galnt11* MO rescue was attempted with *Su(H)-Ank* RNA there was 3.2% abnormal *PitX2* expression (1.6% right, 0% absent, 1.6% bilateral, n = 50). This suggests that knockdown of *Galnt11* can be rescued with *Notch ICD* and *Su(H)-Ank*, both downstream factors of Notch receptor, but cannot be rescued with Delta ligand. The implications from these data are twofold: 1) Since the *Galnt11* MO phenotype cannot be rescued by Delta ligand, Galnt11 and Notch are part of the same pathway, and not two separate parallel pathways, and 2) Galnt11 appears to be acting at the level of Notch receptor.

IV.11. *Galnt11 MO phenotype can be rescued with Notch ICD on the left side*

Given that for normal LR development Galnt11 is required on the left, but not right side, we hypothesized that Notch ICD would preferentially rescue the *Galnt11* MO phenotype when injected on the left side. To test this we injected *Galnt11* MO at the one-cell stage and then co-injected *Notch ICD* RNA together with Alexa Fluor 488 fluorescent tracer in one of two cells at the two-cell stage. The embryos were sorted based on whether *Notch ICD* was injected on the left or right, and they were then evaluated for abnormal *PitX2* expression at the LPM. Embryos that were injected with *Notch ICD* RNA on the right side had 44.4% abnormal *PitX2* expression (7.4% right, 3.7% absent, 33.3% bilateral, n = 67), compared to those injected with *Notch ICD* RNA on the left side, which had 16.7% abnormal *PitX2* expression (0% right, 0% absent, 16.7% bilateral, n = 78) (Fig. 16). UC embryos had

9.1% abnormal *PitX2* expression (1.6% right, 0% absent, 1.6% bilateral, n = 57). This data shows that when *Galnt11* is knocked down, Notch signaling only needs to be upregulated on the left side downstream of Notch receptor. Since Galnt11 appears to only be necessary on the left side for proper heart looping, this further strengthens the argument that Galnt11 and Notch are part of the same pathway.

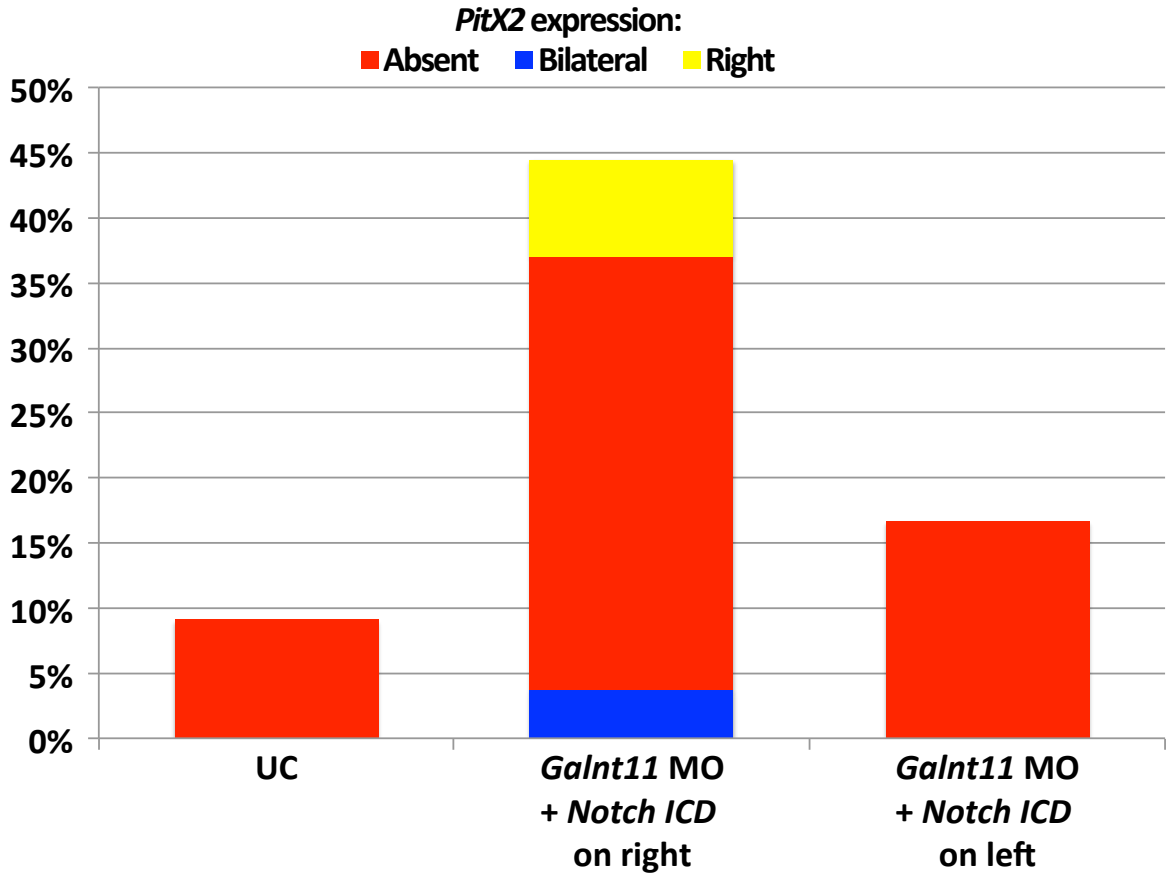

Figure 17. Abnormal *PitX2* expression at the LPM in *Galnt11* morphants can be rescued only when *NotchICD* is injected on the left, but not the right side.

IV.12. *The conserved glycosylation enzymatic domain of Galnt11 is required for proper function*

Galactosyltransferases contain a conserved DSH domain that is essential for their enzymatic function. To further test the hypothesis that Galnt11 glycosylates Notch receptor,

we identified a putative DSH enzymatic domain in Galnt11 and introduced a conservative point mutation from histidine to alanine at amino acid 247. This substitution is predicted to not affect the tertiary structure of Galnt11, and allowed us to test whether the enzymatic galactosyltransferase function of Galnt11 is required for its role in LR development.

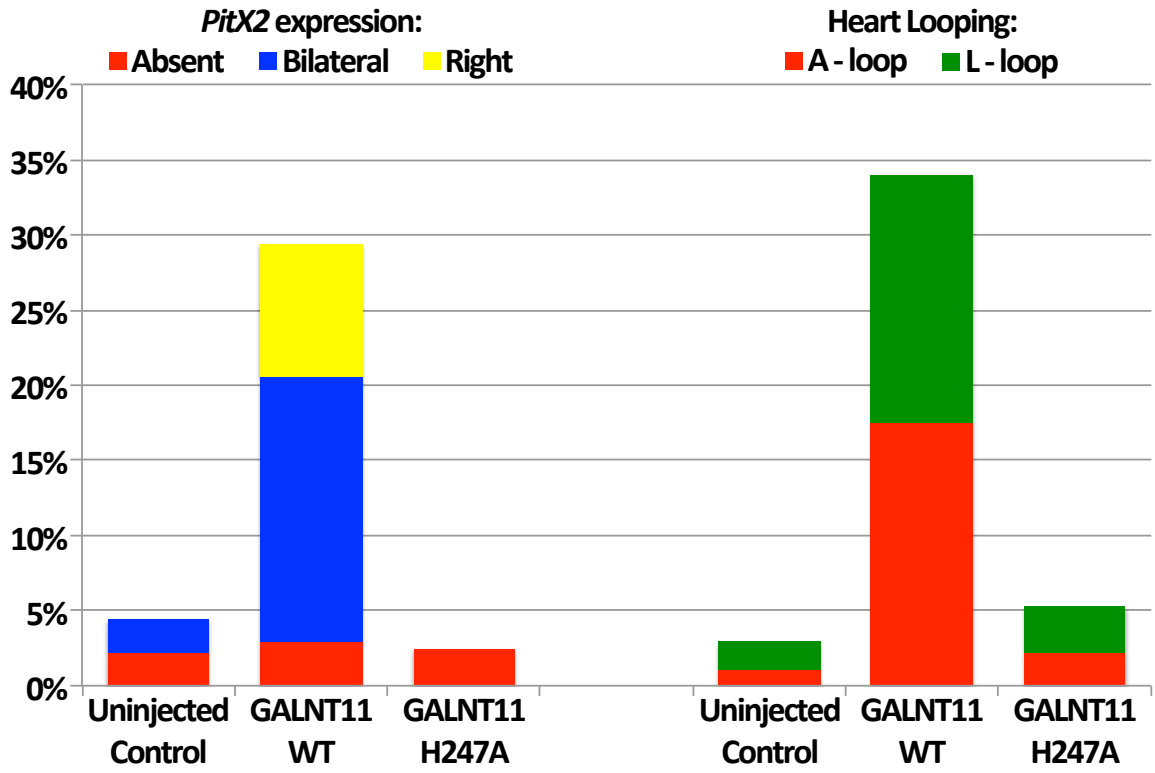

Figure 18. A conservative point mutation in the catalytic glycosylating domain of GALNT11 results in no abnormal heart looping or *PitX2* expression.

We injected one-cell embryos with either wild type (WT) GALNT11 RNA or mutated H247A GALNT11 RNA, and evaluated their *PitX2* expression at the LPM, as well as their heart looping. Consistent with our previous results, UC embryos had 4.4% abnormal *PitX2* expression (0% right, 2.2% absent, 2.2% bilateral, n = 57) and 2.9% abnormal heart looping (1.1% A-loops, 1.8% L-loops, n = 145), while embryos injected with WT GALNT11 RNA had 29.4% abnormal *PitX2* expression (8.8% right, 2.9% absent, 17.6% bilateral, n =

53) and 34.1% abnormal heart looping (17.6% A-loops, 16.5% L-loops, n = 58). However, embryos injected with mutated H247A GALNT11 RNA had 2.5% abnormal *PitX2* expression (0% right, 2.5% absent, 0% bilateral, n = 137) and 5.3% abnormal heart looping (2.3% A-loops, 3.0% L-loops, n = 124), indicating that the DSH catalytic domain of Galnt11 is required to affect asymmetric LR development and further strengthening the argument that Galnt11 and Notch not only act in the same pathways, but that Galnt11 glycosylates Notch.

IV.13. *Galnt11 knockdown and overexpression results in abnormal LRO cilia morphology*

Notch is instrumental in cell-fate specification in many tissues, including the *Xenopus* epidermis where it specifies between ciliated and non-ciliated epidermal cells under the influence of Galnt11. Given that Galnt11 protein is strongly localized at the LRO in crown cells directly surrounding pit cells, we investigated any evidence of cell fate specification changes in the LRO of *Xenopus* embryos injected with *Galnt11* MO. Indeed, the maximal LRO width in *Galnt11* morphants was significantly less than that of control embryos (UC = 181.9 ± 21.4μm vs. *Galnt11* MO = 142.1 ± 29.9μm, $p < 0.0001$), suggesting that Galnt11 controls specification between crown cells and pit cells at the LRO.

IV.14. *Galnt11 affects FoxJ1, and RFX2 expression at the LRO*

Mouse evidence suggests that there are two sets of primary cilia at the LRO, motile and sensory, with motile cilia primarily located in the pit cells and sensory cilia primarily located in the surrounding crown cells. Our evidence indicates that manipulation of *Galnt11* leads to changes in LRO width. To see if these changes in LRO morphology result in changes in cell fate specification, we looked at expression patterns of the motile ciliary genes

FoxJ1 and *RFX2* (Fig. 19). In situ hybridization revealed that compared to UC, both *FoxJ1* and *RFX2* had significantly decreased expression at the LRO in embryos injected with GALNT11 RNA, while *Galnt11* morphants had significantly stronger expression patterns of both genes. Given that immunohistochemistry of the LRO in both overexpressors and morphants of *Galnt11* shows that cilia are present, these results indicate that the fates of these cilia changes with changing levels of *Galnt11.* When overexpressed, motile cilia are suppressed, and when knocked down, motile cilia are upregulated.

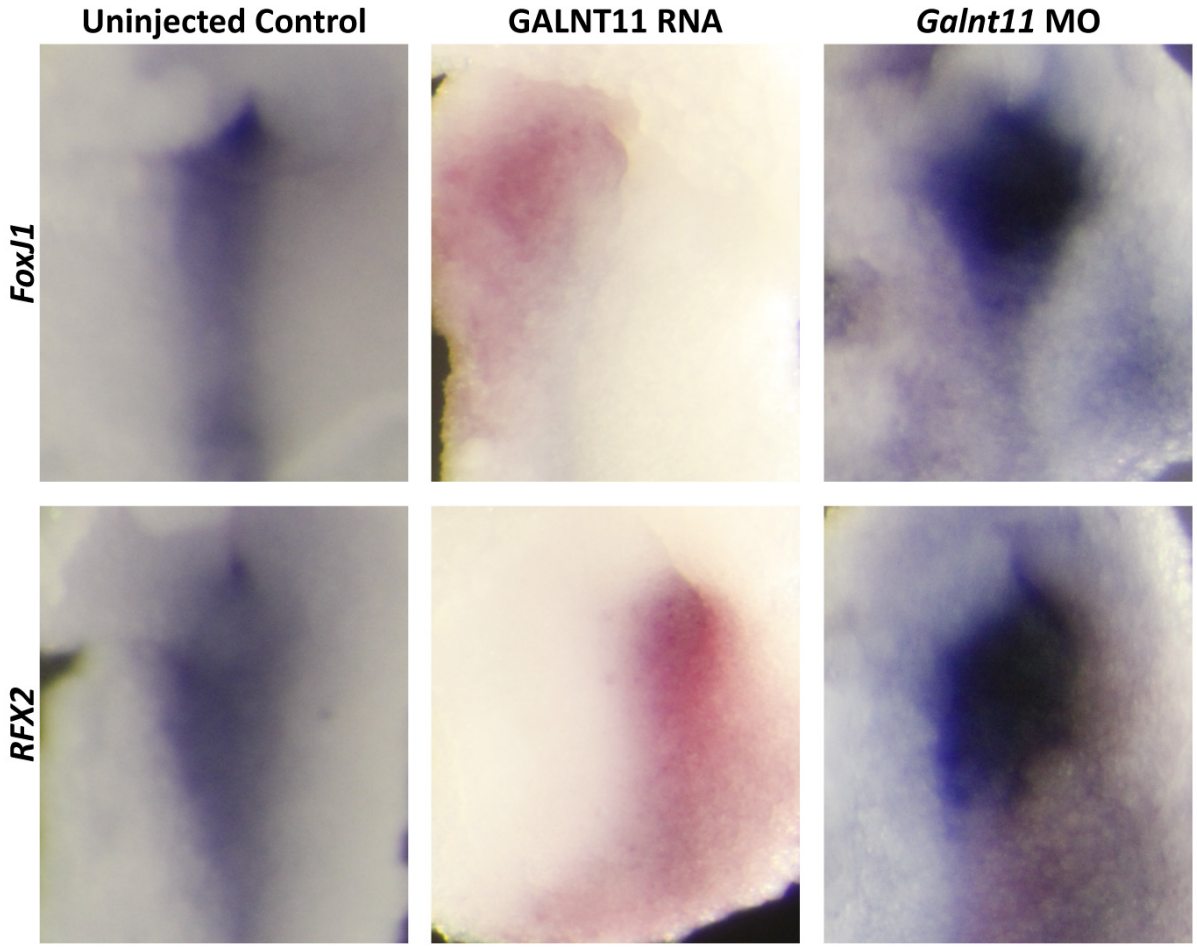

Figure 18. In situ hybridization pictures illustrating that Galnt11 affects ciliary motility genes *FoxJ1* and *RFX2*. With overexpression of *Galnt11*, both *FoxJ1* and *RFX2* expression nearly disappears, while knockdown of *Galnt11* results in much stronger expression of both genes. Gene expression is in blue, while RedGal injection tracer is in red.

V. DISCUSSION

Galnt11 is a previously uncharacterized putative glycosylating agent that was identified through a CNV analysis of patients with heterotaxy. We have shown that Galnt11 is a galactosyltransferase that glycosylates Notch to regulate the development of the LR axis by specifying between motile and sensory ciliary cell fates at the LRO.

V.1. *Galnt11, Notch and LR patterning*

There is extensive evidence that Notch signaling is regulated by glycosylation. Pofut1 is a permissive factor that is required for Notch signaling,[83,84] while Fringe is a modifying factor that can potentiate or attenuate Notch signaling based on the specific ligand/receptor interaction.[98-100] Our data establishes that Galnt11 modifies Notch signaling, but it is unclear whether Galnt11 glycosylation is absolutely necessary for Notch signaling. However, because both knockdown and overexpression of *Galnt11* results in LR axis defects, it appears that Galnt11 is an instructive and not a permissive factor. To our knowledge, Galnt11 is the first enzyme identified to modify Notch with an *N*-galactose sugar. We pinpointed the action of Galnt11 at the level of Notch receptor through a series of epistasis experiments which showed that the *Galnt11* morphant phenotype can be rescued with *NotchICD* and *Su(H)-Ank*, both downstream factors of Notch receptor, but not *Delta*, which is an upstream ligand. Additionally, the lack of phenotype following a conservative mutation of the catalytic domain of Galnt11 indicates that the glycosylating function of Galnt11 is necessary for interaction between the two proteins. Finally, unlike Fringe glycosylation, which only affects Notch inductive signaling, Galnt11 glycosylation appears to also affect lateral inhibition, as

demonstrated by the varying epidermal cilia clump density. To our knowledge Galnt11 is the first non-permissive Notch glycosylation factor to do so.

Previous work implicates Notch signaling at several steps in the LR developmental cascade. Notch is required for peri-LRO expression of *Nodal*,[112,116] and suppression of Notch signaling is necessary for *PitX2* expression at the LPM.[121,152] Data that Notch signaling may be required for *Nodal* expression at the left LPM,[116,122] may influence LRO ciliary length,[115] and may induce asymmetry through asymmetric *Dll1* expression at the LRO is more controversial.[116] Here we show that in addition to regulating the expression of *Nodal* and *PitX2*, Notch is also involved in the specification of motile and sensory cilia at the LRO.

There are several lines of evidence to support this conclusion. Mouse work indicates that mutants that lack motor ciliary components (e.g. dynein motor proteins) develop predominantly either situs solitus or situs inversus,[30,153] while mutants that lack proteins that are required for the formation of cilia in general (e.g. intraflagellar transport proteins) also develop heterotaxy in significant numbers.[13,33,154,155] While not yet demonstrated directly, this difference is presumably because in the case of motor cilia mutants flow is impaired but sensation is intact, and solitus develops based on random fluid perturbations that direct the LR axis towards either SS or SI. It may seem improbable that such small fluid currents would be able to induce the LR cascade, but recent evidence suggests that LRO sensory cilia are sensitive to flow created by as few as two cilia.[156] On the other hand, when all cilia are impaired, no sensory signal of any kind can be transmitted, thus resulting in lack of asymmetric specification and subsequent formation of heterotaxy.

Interestingly, our data shows that manipulations of *Galnt11* can produce both phenotypes. Knockdown produces approximately the same proportion of A- and L-loops,

while overexpression yields almost exclusively L-loops. Mouse data suggests that such phenotypes are consistent with manipulations of motile or sensory cilia at the LRO, and indeed that is what we have found. The alterations in LRO morphology and almost complete absence of motile cilia markers *FoxJ1*, *RFX2* and *DNAH11* in the presence of normal appearing LRO cilia with overexpression of *Galnt11* indicates that there is a decreased number of motile cilia. The alternative case with knockdown of *Galnt11* is more difficult to deduce. Even though the presence of both A-loops and L-loops combined with alterations in LRO morphology and changes in *FoxJ1*, *RFX2* and *DNAH11* suggests a decrease in sensory cilia, to the best of our knowledge there are currently no exclusively sensory cilia markers. Pkd2 has been shown to be involved in the sensation of LRO flow in the mouse, but immunohistochemistry revealed that the channel is present in all LRO cilia, both motile and sensory. Loss of sensory cilia can most directly be demonstrated with a combination of LRO flow analysis and *Coco* expression patterns at the LRO. Since *Coco*, the first gene to become asymmetrically expressed in direct response to LRO flow, has abnormal expression patterns in *Galnt11*/*Notch1* morphants, a demonstration of normal flow would indicate absence of sensory function in the LRO cilia. While we did not perform LRO flow analyses, our epidermal tadpole glide assays show normal epidermal ciliary function in *Galnt11*, indirectly suggesting normal LRO flow function. Epidermal ciliary function has previously been shown to correlate with LRO ciliary flow, suggesting that even though *Galnt11* morphants have appropriate flow, they develop abnormal *Coco* expression patterns (and consequently abnormal LR axis) because of lack of sensory LRO cilia.

Inhibition of Notch signaling by BCL6 and BCoR has recently been shown to be necessary for proper *PitX2* expression at the LPM.[121] This effect appears to be independent

of *Nodal* signaling at the LPM, which is generally thought to be required for *PitX2* expression. Our in situ data supports these results. *Coco* expression patterns are indistinguishable between manipulations of *Galnt11* and *Notch*. However, the *PitX2* expression patterns at the LPM diverge, such that overexpression with GALNT11 RNA results in a significant amount of bilateral *PitX2* expression, while overexpression with *Notch ICD* RNA results in uniformly absent *PitX2* expression. This indicates that even though Notch signaling is involved in the regulation of the LR developmental cascade at multiple steps, Galnt11 only regulates Notch signaling and influences LR development at the level of the ciliated LRO. This is further supported by our in situ and immunohistochemistry data which shows that Galnt11 is present in the LRO, and later in the tadpole kidneys, but not in the LPM.

V.2. *Galnt11 and the genetics of heterotaxy*

Recent advances in genetic analysis, including quantitative interrogation of dense sets of SNPs to identify small CNVs, whole exome sequencing, and as of late whole genome sequencing, have given us the opportunity to investigate the genetic contribution of a variety of complex disease processes. Using such approaches, studies have identified a myriad of potential disease causing genes for conditions as diverse as heterotaxy,[133] congenital diaphragmatic hernias,[157] and hypertension.[158] However, determination of functional significance, if any, of these potential gene candidates is severely complicated by the high degree of locus heterogeneity, tremendous phenotypic variability and incomplete penetrance of the diseases in question.

With our work we clearly demonstrate that model organisms such as *X. tropicalis* provide a powerful tool for functional validation of sequence variants. Previous work in the lab identified 38 small CNVs encompassing 61 potential disease-causing genes.[133] *X. tropicalis* retains substantial synteny to human, and 38 of these identified genes have *X. tropicalis* orthologs (unpublished data). This number is likely to increase, as the *X. tropicalis* genome becomes better assembled. The previous assembly of the genome, for example, yielded only 22 ortholog genes. 7 of those genes were deemed as highly likely to be disease causing, based on expression patterns in the heart or ciliated organs such as the LRO or kidneys. Knockdown of 5 of the 7 genes resulted in heart looping abnormalities, indicating a significant level of functional significance. However, MO knockdown can result in non-specific phenotypes. By delineating in detail the mechanism of action of one of those genes, namely *Galnt11*, we have definitively demonstrated its functional significance in the pathogenesis of heterotaxy.

Generalizing from my work, we our one of the first to demonstrate that novel activities and mechanisms can be a productive of human genetics especially for developmental biology. Traditionally, model organisms have been used to understand developmental processes such as LR patterning and inform us about human development and disease. That approach has been only moderately successful. For example, all of the genes that are currently implicated in LR patterning through the study of mice, chick, rabbit, frog and zebrafish, account for only 10-20% of genetic malformations in patients with heterotaxy.[127,128] Instead, we would argue that aggressive analysis of the genetic variations in patients with congenital malformations such as Htx may be an extraordinary alternative to model system discovery especially since we can directly then address human disease. This

will require forging new alliances between high-throughput model organisms embryologists, clinicians, and human geneticists. The challenges for the human geneticists for studying congenital malformations is not trivial. The genetics of congenital malformations are fraught with locus heterogeneity, complex and variable phenotypes, and relative rarity without extensive pedigrees due to severely reduced fitness that make it very difficult to prove disease causality on the basis of genetic analysis alone. However, the extraordinary power of genome sequencing has simply changed the game making even these complex genetic phenotypes tractable. Also, we anticipate that much of the disease burden is likely to be genetic as opposed to environmental, and the disease is severe so that mutations are not likely to be carried within the populations (ie rare or de novo) which can be used as a powerful filtering method amongst the many variations found in human genomes. Our results would suggest that the genetics can be analyzed and be highly fruitful. Finally, my results would suggest that even rare patients may lead to extraordinary discoveries into the nature of our embryonic development that is critical for our understanding of human disease.

On the other hand, the process of LR patterning also influences how we view human heterotaxy. So far, any malformation of the LR axis in between SS and SI has been simply classified as heterotaxy. The disease specifics are then specified through a description of the macroscopic manifestations, such as left atrial isomerism or isolated dextrocardia with abdominal situs solitus. Our work suggests that heterotaxy is not a single disease process, but rather a group of diseases that all affect LR patterning. With that in mind, we believe that heterotaxy should be redefined based on the genetic abnormality in question, such as cilia motility disorders, cilia sensation disorders, TGF-beta disorders, etc. Data that Down's syndrome patients with AV canal malformations have significantly better short- and

medium-term outcomes compared to non-Down's syndrome patients with AV canal[159] suggests that the specific genetic background of the disease can produce varying outcomes for what appear to be a macroscopically identical disease processes. Classifying heterotaxy patients as suggested may produce similar results and lead to better understanding of prognosis and management. For example, a heterotaxy patient with a sensory cilia malformation is much more likely to have kidney dysfunction than a heterotaxy patient with a TGF-beta mutation affecting Nodal signaling.

Clinically, this has a number of implications. First and foremost, our analysis can provide needed information to families with children that suffer from congenital malformations who often simply want answers. For the first time, we may be able to provide some. Second, by assigning disease causality, we can determine if the mutation is de novo, recessive, or inpenetrant in parents, which will provide critical genetic counseling information. Finally, clearly we are simply scratching the surface of the genes that affect embryonic development. Improving our understanding will surely lead to better prognostication, tailored therapies per genetic lesion, and new drug targets.

VI. REFERENCES

1. Zhu L, Belmont JW, Ware SM. Genetics of human heterotaxias. Eur J Hum Genet 2006;14(1):17–25.

2. Taketazu M, Lougheed J, Yoo S-J, Lim JSL, Hornberger LK. Spectrum of cardiovascular disease, accuracy of diagnosis, and outcome in fetal heterotaxy syndrome. Am J Cardiol 2006;97(5):720–724.

3. Lim JSL, McCrindle BW, Smallhorn JF, et al. Clinical features, management, and outcome of children with fetal and postnatal diagnoses of isomerism syndromes. Circulation 2005;112(16):2454–2461.

4. Raya A, Izpisua Belmonte JC. Left-right asymmetry in the vertebrate embryo: from early information to higher-level integration. Nat Rev Genet 2006;7(4):283–293.

5. Shiratori H, Hamada H. The left-right axis in the mouse: from origin to morphology. Development 2006;133(11):2095–2104.

6. Hirokawa N, Tanaka Y, Okada Y, Takeda S. Nodal flow and the generation of left-right asymmetry. Cell 2006;125(1):33–45.

7. Levin M, Thorlin T, Robinson KR, Nogi T, Mercola M. Asymmetries in H+/K+-ATPase and cell membrane potentials comprise a very early step in left-right patterning. Cell 2002;111(1):77–89.

8. Pagán-Westphal SM, Tabin CJ. The transfer of left-right positional information during chick embryogenesis. Cell 1998;93(1):25–35.

9. Sulik K, Dehart DB, Iangaki T, et al. Morphogenesis of the murine node and notochordal plate. Dev Dyn 1994;201(3):260–278.

10. Essner JJ, Amack JD, Nyholm MK, Harris EB, Yost HJ. Kupffer's vesicle is a ciliated organ of asymmetry in the zebrafish embryo that initiates left-right development of the brain, heart and gut. Development 2005;132(6):1247–1260.

11. Feistel K, Blum M. Three types of cilia including a novel 9+4 axoneme on the notochordal plate of the rabbit embryo. Dev Dyn 2006;235(12):3348–3358.

12. Schweickert A, Weber T, Beyer T, et al. Cilia-driven leftward flow determines laterality in Xenopus. Current Biology 2007;17(1):60–66.

13. Nonaka S, Tanaka Y, Okada Y, et al. Randomization of left-right asymmetry due to loss of nodal cilia generating leftward flow of extraembryonic fluid in mice lacking KIF3B motor protein. Cell 1998;95(6):829–837.

14. Essner JJ, Vogan KJ, Wagner MK, Tabin CJ, Yost HJ, Brueckner M. Conserved function for embryonic nodal cilia. Nature 2002;418(6893):37–38.

15. Blum M, Beyer T, Weber T, et al. Xenopus, an ideal model system to study vertebrate left-right asymmetry. Dev Dyn 2009;238(6):1215–1225.

16. Wilhelmi H. Experimentelle Untersuchungen ueber situs inversus viscerum. 1921;48(1):517–532.

17. Brown NA, Wolpert L. The development of handedness in left/right asymmetry. Development 1990;109(1):1–9.

18. Okada Y, Takeda S, Tanaka Y, Izpisua Belmonte JC, Hirokawa N. Mechanism of nodal flow: a conserved symmetry breaking event in left-right axis determination. Cell 2005;121(4):633–644.

19. Nonaka S, Yoshiba S, Watanabe D, et al. De novo formation of left-right asymmetry by posterior tilt of nodal cilia. PLoS Biol 2005;3(8):e268.

20. Liron N. Stokes flow due to infinite arrays of stokeslets in three dimensions. Journal of engineering mathematics 1996;30(1-2):267–279.

21. Buceta J, Ibañes M, Rasskin-Gutman D, Okada Y, Hirokawa N, Izpisua Belmonte JC. Nodal cilia dynamics and the specification of the left/right axis in early vertebrate embryo development. Biophys J 2005;89(4):2199–2209.

22. Cartwright JHE, Piro N, Piro O, Tuval I. Embryonic nodal flow and the dynamics of nodal vesicular parcels. J R Soc Interface 2007;4(12):49–55.

23. Smith DJ, Gaffney EA, Blake JR. Discrete Cilia Modelling with Singularity Distributions: Application to the Embryonic Node and the Airway Surface Liquid. Bull Math Biol 2007;69(5):1477–1510.

24. Smith DJ, Blake JR, Gaffney EA. Fluid mechanics of nodal flow due to embryonic primary cilia. J R Soc Interface 2008;5(22):567–573.

25. Silverman MA, Leroux MR. Intraflagellar transport and the generation of dynamic, structurally and functionally diverse cilia. Trends Cell Biol 2009;19(7):306–316.

26. Eggenschwiler JT, Anderson KV. Cilia and Developmental Signaling. Annu Rev Cell Dev Biol 2007;23(1):345–373.

27. Caspary T, Larkins CE, Anderson KV. The graded response to Sonic Hedgehog depends on cilia architecture. Dev Cell 2007;12(5):767–778.

28. McGrath J, Somlo S, Makova S, Tian X, Brueckner M. Two populations of node monocilia initiate left-right asymmetry in the mouse. Cell 2003;114(1):61–73.

29. Nauli SM, Alenghat FJ, Luo Y, et al. Polycystins 1 and 2 mediate mechanosensation in the primary cilium of kidney cells. Nat Genet 2003;33(2):129–137.

30. Supp DM, Brueckner M, Kuehn MR, et al. Targeted deletion of the ATP binding domain of left-right dynein confirms its role in specifying development of left-right asymmetries. Development 1999;126(23):5495–5504.

31. Ibañez-Tallon I, Gorokhova S, Heintz N. Loss of function of axonemal dynein Mdnah5 causes primary ciliary dyskinesia and hydrocephalus. Hum Mol Genet 2002;11(6):715–721.

32. Marszalek JR, Ruiz-Lozano P, Roberts E, Chien KR, Goldstein LS. Situs inversus and embryonic ciliary morphogenesis defects in mouse mutants lacking the KIF3A subunit of kinesin-II. Proc Natl Acad Sci USA 1999;96(9):5043–5048.

33. Huangfu D, Liu A, Rakeman AS, Murcia NS, Niswander L, Anderson KV. Hedgehog signalling in the mouse requires intraflagellar transport proteins. Nature 2003;426(6962):83–87.

34. Afzelius BA. A human syndrome caused by immotile cilia. Science 1976;193(4250):317–319.

35. Nonaka S, Shiratori H, Saijoh Y, Hamada H. Determination of left-right patterning of the mouse embryo by artificial nodal flow. Nature 2002;418(6893):96–99.

36. Long S, Ahmad N, Rebagliati M. The zebrafish nodal-related gene southpaw is required for visceral and diencephalic left-right asymmetry. Development 2003;130(11):2303–2316.

37. Levin M, Johnson RL, Stern CD, Kuehn M, Tabin C. A molecular pathway determining left-right asymmetry in chick embryogenesis. Cell 1995;82(5):803–814.

38. Lowe LA, Supp DM, Sampath K, et al. Conserved left-right asymmetry of nodal expression and alterations in murine situs inversus. Nature 1996;381(6578):158–161.

39. Zhou X, Sasaki H, Lowe L, Hogan BL, Kuehn MR. Nodal is a novel TGF-beta-like gene expressed in the mouse node during gastrulation. Nature 1993;361(6412):543–547.

40. Schweickert A, Vick P, Getwan M, et al. The nodal inhibitor Coco is a critical target of leftward flow in Xenopus. Curr Biol 2010;20(8):738–743.

41. Marques S, Borges AC, Silva AC, Freitas S, Cordenonsi M, Belo JA. The activity of the Nodal antagonist Cerl-2 in the mouse node is required for correct L/R body axis. Genes Dev 2004;18(19):2342–2347.

42. Hashimoto H, Rebagliati M, Ahmad N, et al. The Cerberus/Dan-family protein Charon is a negative regulator of Nodal signaling during left-right patterning in zebrafish. Development 2004;131(8):1741–1753.

43. Rodriguez-Esteban C, Capdevila J, Economides AN, Pascual J, Ortiz A, Izpisúa

Belmonte JC. The novel Cer-like protein Caronte mediates the establishment of embryonic left-right asymmetry. Nature 1999;401(6750):243–251.

44. Meno C, Gritsman K, Ohishi S, et al. Mouse Lefty2 and zebrafish antivin are feedback inhibitors of nodal signaling during vertebrate gastrulation. Molecular Cell 1999;4(3):287–298.

45. Cheng AM, Thisse B, Thisse C, Wright CV. The lefty-related factor Xatv acts as a feedback inhibitor of nodal signaling in mesoderm induction and L-R axis development in xenopus. Development 2000;127(5):1049–1061.

46. Bisgrove BW, Essner JJ, Yost HJ. Regulation of midline development by antagonism of lefty and nodal signaling. Development 1999;126(14):3253–3262.

47. Yoshioka H, Meno C, Koshiba K, et al. Pitx2, a bicoid-type homeobox gene, is involved in a lefty-signaling pathway in determination of left-right asymmetry. Cell 1998;94(3):299–305.

48. Ryan AK, Blumberg B, Rodriguez-Esteban C, et al. Pitx2 determines left-right asymmetry of internal organs in vertebrates. Nature 1998;394(6693):545–551.

49. Campione M, Steinbeisser H, Schweickert A, et al. The homeobox gene Pitx2: mediator of asymmetric left-right signaling in vertebrate heart and gut looping. Development 1999;126(6):1225–1234.

50. Morgan TH. The theory of the gene. 1917;51:513–544.

51. Irvine KD, Vogt TF. Dorsal-ventral signaling in limb development. Curr Opin Cell Biol 1997;9(6):867–876.

52. Klein T, Brennan K, Arias AM. An intrinsic dominant negative activity of serrate that is modulated during wing development in Drosophila. Developmental Biology 1997;189(1):123–134.

53. Doherty D, Feger G, Younger-Shepherd S, Jan LY, Jan YN. Delta is a ventral to dorsal signal complementary to Serrate, another Notch ligand, in Drosophila wing formation. Genes Dev 1996;10(4):421–434.

54. Micchelli CA, Rulifson EJ, Blair SS. The function and regulation of cut expression on the wing margin of Drosophila: Notch, Wingless and a dominant negative role for Delta and Serrate. Development 1997;124(8):1485–1495.

55. de Celis JF, Bray S. Feed-back mechanisms affecting Notch activation at the dorsoventral boundary in the Drosophila wing. Development 1997;124(17):3241–3251.

56. Thomas U, Jönsson F, Speicher SA, Knust E. Phenotypic and molecular characterization of SerD, a dominant allele of the Drosophila gene Serrate. Genetics

1995;139(1):203–213.

57. Kim J, Irvine KD, Carroll SB. Cell recognition, signal induction, and symmetrical gene activation at the dorsal-ventral boundary of the developing Drosophila wing. Cell 1995;82(5):795–802.

58. D'Souza B, Meloty-Kapella L, Weinmaster G. Canonical and non-canonical Notch ligands. Curr Top Dev Biol 2010;92:73–129.

59. Gordon WR, Roy M, Vardar-Ulu D, et al. Structure of the Notch1-negative regulatory region: implications for normal activation and pathogenic signaling in T-ALL. Blood 2009;113(18):4381–4390.

60. Logeat F, Bessia C, Brou C, et al. The Notch1 receptor is cleaved constitutively by a furin-like convertase. Proc Natl Acad Sci USA 1998;95(14):8108–8112.

61. Sanchez-Irizarry C, Carpenter AC, Weng AP, Pear WS, Aster JC, Blacklow SC. Notch subunit heterodimerization and prevention of ligand-independent proteolytic activation depend, respectively, on a novel domain and the LNR repeats. Mol Cell Biol 2004;24(21):9265–9273.

62. Nichols JT, Miyamoto A, Weinmaster G. Notch signaling--constantly on the move. Traffic 2007;8(8):959–969.

63. Gordon WR, Vardar-Ulu D, Histen G, Sanchez-Irizarry C, Aster JC, Blacklow SC. Structural basis for autoinhibition of Notch. Nat Struct Mol Biol 2007;14(4):295–300.

64. Windler SL, Bilder D. Endocytic internalization routes required for delta/notch signaling. Curr Biol 2010;20(6):538–543.

65. Zolkiewska A. ADAM proteases: ligand processing and modulation of the Notch pathway. Cell Mol Life Sci 2008;65(13):2056–2068.

66. Selkoe DJ, Wolfe MS. Presenilin: running with scissors in the membrane. Cell 2007;131(2):215–221.

67. Wolfe MS, Kopan R. Intramembrane proteolysis: theme and variations. Science 2004;305(5687):1119–1123.

68. Kao HY, Ordentlich P, Koyano-Nakagawa N, et al. A histone deacetylase corepressor complex regulates the Notch signal transduction pathway. Genes Dev 1998;12(15):2269–2277.

69. Jarriault S, Brou C, Logeat F, Schroeter EH, Kopan R, Israël A. Signalling downstream of activated mammalian Notch. Nature 1995;377(6547):355–358.

70. Bailey AM, Posakony JW. Suppressor of hairless directly activates transcription of

enhancer of split complex genes in response to Notch receptor activity. Genes Dev 1995;9(21):2609–2622.

71. Bray S, Furriols M. Notch pathway: making sense of suppressor of hairless. Current Biology 2001;11(6):R217–21.

72. Flores GV, Duan H, Yan H, et al. Combinatorial signaling in the specification of unique cell fates. Cell 2000;103(1):75–85.

73. Artavanis-Tsakonas S, Rand MD, Lake RJ. Notch signaling: cell fate control and signal integration in development. Science 1999;284(5415):770–776.

74. Bray S. Notch signalling in Drosophila: three ways to use a pathway. Seminars in Cell and Developmental Biology 1998;9(6):591–597.

75. Panin VM, Irvine KD. Modulators of Notch signaling. Seminars in Cell and Developmental Biology 1998;9(6):609–617.

76. Justice NJ, Jan YN. Variations on the Notch pathway in neural development. Curr Opin Neurobiol 2002;12(1):64–70.

77. Haines N, Irvine KD. Glycosylation regulates Notch signalling. Nat Rev Mol Cell Biol 2003;4(10):786–797.

78. Irvine KD. Fringe, Notch, and making developmental boundaries. Current opinion in genetics & development 1999;9(4):434–441.

79. Haltiwanger RS, Stanley P. Modulation of receptor signaling by glycosylation: fringe is an O-fucose-beta1,3-N-acetylglucosaminyltransferase. Biochim Biophys Acta 2002;1573(3):328–335.

80. Haltiwanger RS. Regulation of signal transduction pathways in development by glycosylation. Curr Opin Struct Biol 2002;12(5):593–598.

81. Harris RJ, Spellman MW. O-linked fucose and other post-translational modifications unique to EGF modules. Glycobiology 1993;3(3):219–224.

82. Moloney DJ, Shair LH, Lu FM, et al. Mammalian Notch1 is modified with two unusual forms of O-linked glycosylation found on epidermal growth factor-like modules. J Biol Chem 2000;275(13):9604–9611.

83. Wang Y, Spellman MW. Purification and characterization of a GDP-fucose:polypeptide fucosyltransferase from Chinese hamster ovary cells. J Biol Chem 1998;273(14):8112–8118.

84. Wang Y, Shao L, Shi S, et al. Modification of epidermal growth factor-like repeats with O-fucose. Molecular cloning and expression of a novel GDP-fucose protein O-fucosyltransferase. J Biol Chem 2001;276(43):40338–40345.

85. Wang Y, Lee GF, Kelley RF, Spellman MW. Identification of a GDP-L-fucose:polypeptide fucosyltransferase and enzymatic addition of O-linked fucose to EGF domains. Glycobiology 1996;6(8):837–842.

86. Panin VM, Shao L, Lei L, Moloney DJ, Irvine KD, Haltiwanger RS. Notch ligands are substrates for protein O-fucosyltransferase-1 and Fringe. J Biol Chem 2002;277(33):29945–29952.

87. Shao L, Moloney DJ, Haltiwanger R. Fringe modifies O-fucose on mouse Notch1 at epidermal growth factor-like repeats within the ligand-binding site and the Abruptex region. J Biol Chem 2003;278(10):7775–7782.

88. Moloney DJ, Panin VM, Johnston SH, et al. Fringe is a glycosyltransferase that modifies Notch. Nature 2000;406(6794):369–375.

89. Chen J, Moloney DJ, Stanley P. Fringe modulation of Jagged1-induced Notch signaling requires the action of beta 4galactosyltransferase-1. Proc Natl Acad Sci USA 2001;98(24):13716–13721.

90. Okajima T, Irvine KD. Regulation of notch signaling by o-linked fucose. Cell 2002;111(6):893–904.

91. Sasamura T, Sasaki N, Miyashita F, et al. neurotic, a novel maternal neurogenic gene, encodes an O-fucosyltransferase that is essential for Notch-Delta interactions. Development 2003;130(20):4785–4795.

92. Okajima T, Xu A, Irvine KD. Modulation of notch-ligand binding by protein O-fucosyltransferase 1 and fringe. J Biol Chem 2003;278(43):42340–42345.

93. Oka C, Nakano T, Wakeham A, et al. Disruption of the mouse RBP-J kappa gene results in early embryonic death. Development 1995;121(10):3291–3301.

94. Herreman A, Hartmann D, Annaert W, et al. Presenilin 2 deficiency causes a mild pulmonary phenotype and no changes in amyloid precursor protein processing but enhances the embryonic lethal phenotype of presenilin 1 deficiency. Proc Natl Acad Sci USA 1999;96(21):11872–11877.

95. Donoviel DB, Hadjantonakis AK, Ikeda M, Zheng H, Hyslop PS, Bernstein A. Mice lacking both presenilin genes exhibit early embryonic patterning defects. Genes Dev 1999;13(21):2801–2810.

96. Shi S, Stanley P. Protein O-fucosyltransferase 1 is an essential component of Notch signaling pathways. Proc Natl Acad Sci USA 2003;100(9):5234–5239.

97. Yuan YP, Schultz J, Mlodzik M, Bork P. Secreted fringe-like signaling molecules may be glycosyltransferases. Cell 1997;88(1):9–11.

98. Panin VM, Papayannopoulos V, Wilson R, Irvine KD. Fringe modulates Notch-

ligand interactions. Nature 1997;387(6636):908–912.

99. Fleming RJ, Gu Y, Hukriede NA. Serrate-mediated activation of Notch is specifically blocked by the product of the gene fringe in the dorsal compartment of the Drosophila wing imaginal disc. Development 1997;124(15):2973–2981.

100. Klein T, Arias AM. Interactions among Delta, Serrate and Fringe modulate Notch activity during Drosophila wing development. Development 1998;125(15):2951–2962.

101. Moloney DJ, Lin AI, Haltiwanger RS. The O-linked fucose glycosylation pathway. Evidence for protein-specific elongation of o-linked fucose in Chinese hamster ovary cells. J Biol Chem 1997;272(30):19046–19050.

102. Bruckner K, Perez L, Clausen H, Cohen S. Glycosyltransferase activity of Fringe modulates Notch-Delta interactions. Nature 2000;406(6794):411–415.

103. Shao L, Luo Y, Moloney DJ, Haltiwanger R. O-glycosylation of EGF repeats: identification and initial characterization of a UDP-glucose: protein O-glucosyltransferase. Glycobiology 2002;12(11):763–770.

104. Wiggins CA, Munro S. Activity of the yeast MNN1 alpha-1,3-mannosyltransferase requires a motif conserved in many other families of glycosyltransferases. Proc Natl Acad Sci USA 1998;95(14):7945–7950.

105. Munro S, Freeman M. The notch signalling regulator fringe acts in the Golgi apparatus and requires the glycosyltransferase signature motif DXD. Current Biology 2000;10(14):813–820.

106. Selva EM, Hong K, Baeg GH, et al. Dual role of the fringe connection gene in both heparan sulphate and fringe-dependent signalling events. Nat Cell Biol 2001;3(9):809–815.

107. Goto S, Taniguchi M, Muraoka M, et al. UDP-sugar transporter implicated in glycosylation and processing of Notch. Nat Cell Biol 2001;3(9):816–822.

108. Hicks C, Johnston SH, diSibio G, Collazo A, Vogt TF, Weinmaster G. Fringe differentially modulates Jagged1 and Delta1 signalling through Notch1 and Notch2. Nat Cell Biol 2000;2(8):515–520.

109. Shimizu K, Chiba S, Saito T, Kumano K, Takahashi T, Hirai H. Manic fringe and lunatic fringe modify different sites of the Notch2 extracellular region, resulting in different signaling modulation. J Biol Chem 2001;276(28):25753–25758.

110. Jacobsen TL, Brennan K, Arias AM, Muskavitch MA. Cis-interactions between Delta and Notch modulate neurogenic signalling in Drosophila. Development 1998;125(22):4531–4540.

111. Irvine KD, Rauskolb C. Boundaries in development: formation and function. Annu Rev Cell Dev Biol 2001;17:189–214.

112. Krebs LT, Iwai N, Nonaka S, et al. Notch signaling regulates left-right asymmetry determination by inducing Nodal expression. Genes Dev 2003;17(10):1207–1212.

113. Takeuchi JK, Lickert H, Bisgrove BW, et al. Baf60c is a nuclear Notch signaling component required for the establishment of left-right asymmetry. Proc Natl Acad Sci USA 2007;104(3):846–851.

114. Przemeck GKH, Heinzmann U, Beckers J, Hrabé de Angelis M. Node and midline defects are associated with left-right development in Delta1 mutant embryos. Development 2003;130(1):3–13.

115. Lopes SS, Lourenco R, Pacheco L, Moreno N, Kreiling J, Saude L. Notch signalling regulates left-right asymmetry through ciliary length control. Development 2010;137(21):3625–3632.

116. Raya A, Kawakami Y, Rodríguez-Esteban C, et al. Notch activity induces Nodal expression and mediates the establishment of left-right asymmetry in vertebrate embryos. Genes Dev 2003;17(10):1213–1218.

117. Brennan J, Norris DP, Robertson EJ. Nodal activity in the node governs left-right asymmetry. Genes Dev 2002;16(18):2339–2344.

118. Saijoh Y, Oki S, Ohishi S, Hamada H. Left-right patterning of the mouse lateral plate requires nodal produced in the node. Developmental Biology 2003;256(1):160–172.

119. Adachi H, Saijoh Y, Mochida K, et al. Determination of left/right asymmetric expression of nodal by a left side-specific enhancer with sequence similarity to a lefty-2 enhancer. Genes Dev 1999;13(12):1589–1600.

120. Norris DP, Robertson EJ. Asymmetric and node-specific nodal expression patterns are controlled by two distinct cis-acting regulatory elements. Genes Dev 1999;13(12):1575–1588.

121. Sakano D, Kato A, Parikh N, et al. BCL6 canalizes Notch-dependent transcription, excluding Mastermind-like1 from selected target genes during left-right patterning. Dev Cell 2010;18(3):450–462.

122. Gourronc F, Ahmad N, Nedza N, Eggleston T, Rebagliati M. Nodal activity around Kupffer's vesicle depends on the T-box transcription factors Notail and Spadetail and on Notch signaling. Dev Dyn 2007;236(8):2131–2146.

123. Hojo M, Takashima S, Kobayashi D, et al. Right-elevated expression of charon is regulated by fluid flow in medaka Kupffer's vesicle. Dev Growth Differ 2007;49(5):395–405.

124. Raya A, Kawakami Y, Rodríguez-Esteban C, et al. Notch activity acts as a sensor for extracellular calcium during vertebrate left-right determination. Nature 2004;427(6970):121–128.

125. Anagnostopoulos PV, Pearl JM, Octave C, et al. Improved current era outcomes in patients with heterotaxy syndromes. Eur J Cardiothorac Surg 2009;35(5):871–7; discussion 877–8.

126. Cohen MS, Anderson RH, Cohen MI, et al. Controversies, genetics, diagnostic assessment, and outcomes relating to the heterotaxy syndrome. Cardiol Young 2007;17 Suppl 2:29–43.

127. Belmont JW, Mohapatra B, Towbin JA, Ware SM. Molecular genetics of heterotaxy syndromes. Curr Opin Cardiol 2004;19(3):216–220.

128. Sutherland MJ, Ware SM. Disorders of Left-Right Asymmetry: Heterotaxy and Situs Inversus. Am J Med Genet C 2009;151C(4):307–317.

129. Kennedy MP, Omran H, Leigh MW, et al. Congenital heart disease and other heterotaxic defects in a large cohort of patients with primary ciliary dyskinesia. Circulation 2007;115(22):2814–2821.

130. Quinlan RJ, Tobin JL, Beales PL. Modeling ciliopathies: Primary cilia in development and disease. Curr Top Dev Biol 2008;84:249–310.

131. Ruiz-Perez VL, Goodship JA. Ellis-van Creveld syndrome and Weyers acrodental dysostosis are caused by cilia-mediated diminished response to hedgehog ligands. Am J Med Genet C 2009;151C(4):341–351.

132. Chung B, Shaffer LG, Keating S, Johnson J, Casey B, Chitayat D. From VACTERL-H to heterotaxy: variable expressivity of ZIC3-related disorders. Am J Med Genet A 2011;155A(5):1123–1128.

133. Fakhro KA, Choi M, Ware SM, et al. Rare copy number variations in congenital heart disease patients identify unique genes in left-right patterning. Proc Natl Acad Sci USA 2011;108(7):2915–2920.

134. Hellsten U, Harland RM, Gilchrist MJ, et al. The genome of the Western clawed frog Xenopus tropicalis. Science 2010;328(5978):633–636.

135. Hanisch FG. O-Glycosylation of the mucin type. Biological chemistry 2001;382(2):143–149.

136. Hang HC, Bertozzi CR. The chemistry and biology of mucin-type O-linked glycosylation. Bioorg Med Chem 2005;13(17):5021–5034.

137. Brockhausen I. Mucin-type O-glycans in human colon and breast cancer: glycodynamics and functions. EMBO Rep 2006;7(6):599–604.

138. Tarp MA, Clausen H. Mucin-type O-glycosylation and its potential use in drug and vaccine development. Biochim Biophys Acta 2008;1780(3):546–563.

139. Clausen H, Bennett EP. A family of UDP-GalNAc: polypeptide N-acetylgalactosaminyl-transferases control the initiation of mucin-type O-linked glycosylation. Glycobiology 1996;6(6):635–646.

140. Hagen Ten KG, Fritz TA, Tabak LA. All in the family: the UDP-GalNAc:polypeptide N-acetylgalactosaminyltransferases. Glycobiology 2003;13(1):1R–16R.

141. Tian E, Hagen Ten KG. Recent insights into the biological roles of mucin-type O-glycosylation. Glycoconj J 2009;26(3):325–334.

142. Hagen Ten KG, Tran DT, Gerken TA, Stein DS, Zhang Z. Functional characterization and expression analysis of members of the UDP-GalNAc:polypeptide N-acetylgalactosaminyltransferase family from Drosophila melanogaster. J Biol Chem 2003;278(37):35039–35048.

143. Topaz O, Shurman DL, Bergman R, et al. Mutations in GALNT3, encoding a protein involved in O-linked glycosylation, cause familial tumoral calcinosis. Nat Genet 2004;36(6):579–581.

144. Kato K, Jeanneau C, Tarp MA, et al. Polypeptide GalNAc-transferase T3 and familial tumoral calcinosis. Secretion of fibroblast growth factor 23 requires O-glycosylation. J Biol Chem 2006;281(27):18370–18377.

145. Kathiresan S, Melander O, Guiducci C, et al. Six new loci associated with blood low-density lipoprotein cholesterol, high-density lipoprotein cholesterol or triglycerides in humans. Nat Genet 2008;40(2):189–197.

146. Willer CJ, Sanna S, Jackson AU, et al. Newly identified loci that influence lipid concentrations and risk of coronary artery disease. Nat Genet 2008;40(2):161–169.

147. Teslovich TM, Musunuru K, Smith AV, et al. Biological, clinical and population relevance of 95 loci for blood lipids. Nature 2010;466(7307):707–713.

148. Schjoldager KT-BG, Vester-Christensen MB, Bennett EP, et al. O-glycosylation modulates proprotein convertase activation of angiopoietin-like protein 3: possible role of polypeptide GalNAc-transferase-2 in regulation of concentrations of plasma lipids. Journal of Biological Chemistry 2010;285(47):36293–36303.

149. Miwa HE, Gerken TA, Jamison O, Tabak LA. Isoform-specific O-glycosylation of osteopontin and bone sialoprotein by polypeptide N-acetylgalactosaminyltransferase-1. Journal of Biological Chemistry 2010;285(2):1208–1219.

150. Zhang L, Tran DT, Hagen Ten KG. An O-glycosyltransferase promotes cell adhesion during development by influencing secretion of an extracellular matrix

integrin ligand. Journal of Biological Chemistry 2010;285(25):19491–19501.

151. Khokha MK, Chung C, Bustamante EL, et al. Techniques and probes for the study of Xenopus tropicalis development. Dev Dyn 2002;225(4):499–510.

152. Hilton EN, Manson FDC, Urquhart JE, et al. Left-sided embryonic expression of the BCL-6 corepressor, BCOR, is required for vertebrate laterality determination. Hum Mol Genet 2007;16(14):1773–1782.

153. Supp DM, Witte DP, Potter SS, Brueckner M. Mutation of an axonemal dynein affects left-right asymmetry in inversus viscerum mice. Nature 1997;389(6):963–966.

154. García-García MJ, Eggenschwiler JT, Caspary T, et al. Analysis of mouse embryonic patterning and morphogenesis by forward genetics. Proc Natl Acad Sci USA 2005;102(17):5913–5919.

155. Murcia NS, Richards WG, Yoder BK, Mucenski ML, Dunlap JR, Woychik RP. The Oak Ridge Polycystic Kidney (orpk) disease gene is required for left-right axis determination. Development 2000;127(11):2347–2355.

156. Kawasumi A, Takamatsu A, Yoshiba S, et al. Two rotating cilia in the node cavity are sufficient to break left–right symmetry in the mouse embryo. Nature Communications 2011;3:622–8.

157. Kantarci S, Ackerman KG, Russell MK, et al. Characterization of the chromosome 1q41q42.12 region, and the candidate gene DISP1, in patients with CDH. Am J Med Genet A 2010;152A(10):2493–2504.

158. Boyden LM, Choi M, Choate KA, et al. Mutations in kelch-like 3 and cullin 3 cause hypertension and electrolyte abnormalities. Nature 2012;482(7383):98–102.

159. Formigari R, Di Donato RM, Gargiulo G, et al. Better surgical prognosis for patients with complete atrioventricular septal defect and Down's syndrome. Ann Thorac Surg 2004;78(2):666–72; discussion 672.